inorganics

MDPI

Review

Bio-Inspired Synthesis of Carbon-Based Nanomaterials and Their Potential Environmental Applications: A State-of-the-Art Review

Vishal Dutta [1], Ritesh Verma [2], C. Gopalkrishnan [3], Min-Hao Yuan [4,*], Khalid Mujasam Batoo [5], R. Jayavel [6], Ankush Chauhan [7,*], Kun-Yi Andrew Lin [8], Ravindran Balasubramani [9,10] and Suresh Ghotekar [11,*]

1 School of Advanced Chemical Sciences, Shoolini University, Solan 173212, Himachal Pradesh, India
2 University Centre for Research and Development, Chandigarh University, Mohali 140413, Punjab, India
3 Department of Physics and Nanotechnology, SRM Institute of Science and Technology, Chennai 603203, Tamil Nadu, India
4 Department of Occupational Safety and Health, China Medical University, Taichung 406, Taiwan
5 King Abdullah Institute for Nanotechnology, King Saud University, P.O. Box 2455, Riyadh 11451, Saudi Arabia
6 Centre for Nanoscience and Technology, Anna University, Chennai 600025, Tamil Nadu, India
7 Faculty of Allied Health Sciences, Chettinad Academy of Research and Education, Chettinad Hospital and Research Institute, Kelambakkam, Chennai 603103, Tamil Nadu, India
8 Department of Environmental Engineering & Innovation and Development Center of Sustainable Agriculture, National Chung Hsing University, 250 Kuo-Kuang Road, Taichung 402, Taiwan
9 Department of Medical Biotechnology and Integrative Physiology, Institute of Biotechnology, Saveetha School of Engineering, Saveetha Institute of Medical and Technical Sciences, Thandalam, Chennai 602105, Tamil Nadu, India
10 Department of Environmental Energy and Engineering, Kyonggi University, Yeongtong-gu, Suwon 16227, Gyeonggi-do, Korea
11 Department of Chemistry, Smt. Devkiba Mohansinhji Chauhan College of Commerce and Science, University of Mumbai, Silvassa 396230, Dadra and Nagar Haveli (UT), India
* Correspondence: mhyuan@mail.cmu.edu.tw (M.-H.Y.); ankushchauhan18@gmail.com (A.C.); ghotekarsuresh7@gmail.com (S.G.)

Abstract: Providing safe drinking water and clean water is becoming a more challenging task all around the world. Although some critical issues and limits remain unsolved, implementing ecologically sustainable nanomaterials (NMs) with unique features, e.g., highly efficient and selective, earth-abundance, renewability, low-cost manufacturing procedures, and stability, has become a priority. Carbon nanoparticles (NPs) offer tremendous promise in the sectors of energy and the environment. However, a series of far more ecologically friendly synthesis techniques based on natural, renewable, and less expensive waste resources must be explored. This will reduce greenhouse gas emissions and harmful material extraction and assist the development of green technologies. The progress achieved in the previous 10 years in the fabrication of novel carbon-based NMs utilizing waste materials as well as natural precursors is reviewed in this article. Research on carbon-based NPs and their production using naturally occurring precursors and waste materials focuses on this review research. Water treatment and purification using carbon NMs, notably for industrial and pharmaceutical wastes, has shown significant potential. Research in this area focuses on enhanced carbonaceous NMs, methods, and novel nano-sorbents for wastewater, drinking water, groundwater treatment, as well as ionic metal removal from aqueous environments. Discussed are the latest developments and challenges in environmentally friendly carbon and graphene quantum dot NMs.

Keywords: carbon nanomaterials; green synthesis; water treatment; environmental remediation; multifunctional applications

Citation: Dutta, V.; Verma, R.; Gopalkrishnan, C.; Yuan, M.-H.; Batoo, K.M.; Jayavel, R.; Chauhan, A.; Lin, K.-Y.A.; Balasubramani, R.; Ghotekar, S. Bio-Inspired Synthesis of Carbon-Based Nanomaterials and Their Potential Environmental Applications: A State-of-the-Art Review. *Inorganics* **2022**, *10*, 169. https://doi.org/10.3390/inorganics10100169

Academic Editors: Alejandro Pérez-Larios and Oomman K. Varghese

Received: 9 August 2022
Accepted: 23 September 2022
Published: 10 October 2022

1. Introduction

Undoubtedly, environmental contamination is one of the most serious issues confronting civilization today [1]. Thousands of tons of harmful chemicals are dumped into lakes, rivers, and seas every day. Heavy metals, textile dyes, herbicides, surfactants, and insecticides are examples of harmful contaminants found in the aquatic environment [2]. The removal of these harmful and poisonous pollutants from water bodies has received considerable attention in order to prevent their hazardous impact on the planet [3]. Day by day, new approaches are continually being investigated to remove toxins present in the air, water, and soil. In addition, due to the fast population increase, medications are used extensively in health care, and a considerable amount of these substances are pumped into the environment in decomposed or untapped forms [4,5]. As a result of the continuous enhancement in people's housing conditions and the quick introduction of industrialization, humankind in the twenty-first century has confronted environmental challenges resulting from natural resource pollution. As a result, mineralization, eradication, conversion, and reduction of pollution molecules from the aquatic environment are sorely needed [6]. Furthermore, the world's energy needs are mostly addressed by fossil fuels such as petroleum, natural gas, and coal, which are rapidly diminishing. One of the most significant challenges is the persistently increasing concentration of CO_2, the main greenhouse gas available in the atmosphere, as a result of rapid industrialization and excessive fossil fuel burning. Anthropogenic CO_2 emissions have considerably impacted on global climate change as a greenhouse gas. In this context, researchers consider the best techniques for overcoming the mentioned problems [7–9]. Water purification techniques have been extensively developed in chemical, coagulation, flotation, sedimentation, biological, physical, gravity separation, reverse osmosis, and filtration. However, due to the movement of pollutants from one phase to another or partial removal, the performance of these technologies is not particularly good for effectively cleaning polluted water [10–13]. Nanotechnology has picked much attention in recent years due to the remarkable physicochemical characteristics of nanomaterials (NMs) [14–16]. NMs have a higher surface-to-volume ratio than their bulkier competitors, resulting in increased reactivity and greater efficacy. In addition, compared to traditional techniques, NMs have the potential to leverage unique surface chemistry, enabling them to be synthesized and characterized or patched with functional groups which can target specific molecules of concerned pollutants for effective remediation of the environment [17,18]. Furthermore, systematic modification of nanoparticles' (NPs) physical properties (such as size, shape, permeability, and chemical composition) may convey additional favorable qualities that ultimately enhance the material's effectiveness for pollutant treatment. The wide surface modification chemistry of the NMs and its adjustable physicochemical parameters offer significant advantages over standard techniques associated with environmental contamination [19,20]. As a result, technologies that integrate multiple diverse materials (hybrids/nano-composites) to harvest desirable characteristics from each component are more economical, efficient, and durable than approaches focused on a particular nanotechnology field [21]. When compared to NPs alone, anchoring NPs to a framework is always an alternative approach to enhance the material's sustainability [22]. NMs that have been functionalized with certain chemicals that target contaminant molecules of concern can enhance the specificity and effectiveness of NMs [23,24]. The NMs utilized to clean up pollution must not be another pollutant once they have been utilized. As a result, biodegradable materials are especially appealing in this environmental application field. Biodegradable NMs will enhance consumer trust and acceptance of technology by removing the need to dispose of material waste after treatment and providing a greener and safer approach for pollution remediation in the environment [25,26]. Additionally, emerging technologies that rely on the absorption of pollutants on a target-specific basis are particularly appealing because they address poor efficiency imposed by off-targeting. As a consequence, several studies have focused on integrating nanotechnology principles with the chemical and physical surface modification of NMs to obtain engineered NMs that can conquer several of the issues encountered during

contamination remediation [27–29]. Some key challenges that must be considered when developing new NMs for environmental remediation include target-specific identification, facile and economical fabrication, non-toxic nature, biocompatible, reusability, and the ability for regeneration after use [30–36].

Whereas numerous "nano" forms of carbon are becoming increasingly popular over the years and are being vigorously explored more than ever around the world, which is certainly justified due to their incredible characteristics, one should not underestimate the astounding range of technological solutions that bio-based carbons can deliver [37–40]. Exclusively, the gigantic majority of porous carbons are considered those are cost-effective and display potential for environmental prominence. Porous carbons, for comparison purposes, are often used in industrial applications and have always been the subject of extensive interest in categories, such as gas storage [41], heat management [42], compression [43], detection and separation [44], solar energy storage [45], supercapacitors [46], electrochemical energy storage and conversion [47], batteries and fuel cells [48,49], catalysis [50,51], pollutants elimination in gas as well as liquid [52,53], photocatalysis [54–56], and protection against electromagnetic waves [57]. Interestingly, 62.1% of published data comprise the practical application and designing of carbon-based NMs for water mitigation practice (Figure 1a). Considering the significance of porous materials, the demand for natural, recyclable, low-cost, yet efficient precursors promises to be a worthwhile endeavor. Because of the wide range of potential compositions and porosity scales involved, bio-based raw materials can be considered for all of the uses as mentioned above [58]. Carbon includes a broad range of allotropic forms, ranging from 0-D to 3-D nano-structures, whereas some of the forms, such as graphene and its derivatives, are rising in popularity, especially when novel features are found and exploited in the introduction of unique functional NMs for environmental applications [59]. A survey based on carbon NPs exemplifies that from 2012 to 2021, searching the keywords "carbon nanoparticles for environmental remediation" displays approximately 10,500 publications. This depicts the keen apprehension of the scientific community for remediation of the environment via carbon-based NPs (Figure 1b). The present review comprehensively represents and encourages the scientific community to go further than traditional approaches and reconsider the primordial carbon forms in new green technologies for eco-friendly environmental applications. The significant aspect of the research represented in this review portrays the green fabrication of carbon-based NMs and highlights a huge spectrum of carbon-based NMs for a wide range of environmental uses.

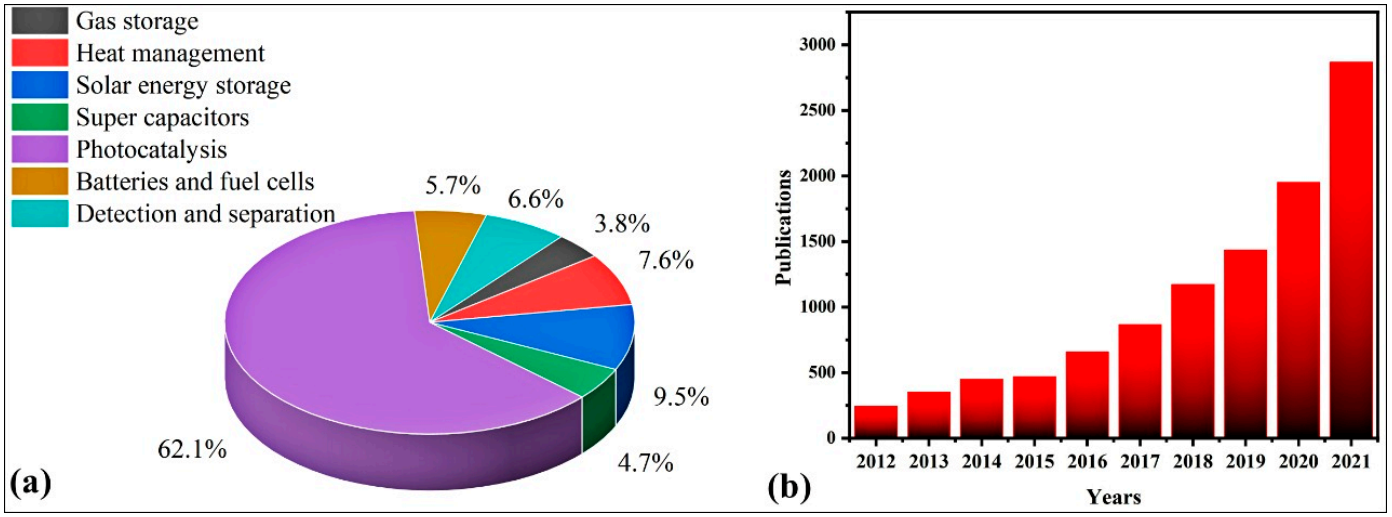

Figure 1. (**a**) Diverse environmental applications of carbon-based NMs (Scopus searched) (**b**) Publications from 2012 to 2021 searched on dated 4 April 2022 employing keyword "carbon-based nanoparticles + environment mitigation.

2. Carbon Nanoparticles as a Promising Future Nanomaterial

Certainly, various innovative carbon-based NMs have been utilized to construct cost-effective techniques and slightly elevated water purification systems for real-time and continuous environmental monitoring; such NPs have also been widely used for effluent remediation, mitigation, and purification [60]. Carbon NMs are easily recyclable. They also efficiently preserve the water quality for quite a long time, are convenient, and demonstrate practicability of water supply while repetitively detecting biological and chemical pollution from synthetic, municipal, and industrial water waste [61]. This sub-part represents the potential of carbon NMs for future environmental treatment. Carbon-based NPs, such as carbon nanotubes (CNTs), carbon quantum dots (CQDs), graphene, and other derivatives, are used for the remediation of water and elimination of pharmaceutical waste as well [62,63]. Carbon NPs possess a number of unique forms and characteristics that are intimately connected to the carbon atom's distinctive atomic structure. Carbon NPs are classified as zero-dimensional NPs (such as fullerenes and carbon quantum dots), 1-D NPs (such as carbon nanotubes and carbon nanofibers), 2-D NPs (graphene), and 3-D NPs (like carbon sponges) based on their distinctive dimensionality, morphology and size [64,65]. The most prominent 1-D carbon nanostructures are carbon nanotubes (CNTs) and carbon nanofibers. These carbon nanostructures are formed from rounded graphene sheets. Carbon nanotubes (CNTs) also possess a tube-like shape. Once carbon nanotubes (CNTs) are formed, the other derivatives, such as single-walled, double-walled and multi-walled carbon nanotubes are formed from them [66]. Recent studies also reported that CNTs could also efficiently eliminate metal ions such as chromium (III) as well as pharmaceutical wastes from water [67]. As per the demand for modern approaches, CNTs possess tunable characteristics, having exceptional mechanical strength and chemical stability, making them excellent contenders for a broad range of uses. Due to the astoundingly high surface-to-area ratio, improved chemical stability, cost-effective and limited effect on the environment that carbon-based NPs have, they are a great alternative for the degradation of environmental issues [68]. CNTs and allotropes with a cylindrical nanostructure are excellent nano-sorbents for the decomposition of diverse pollutants and could be used to remove pharma pollutants or their byproducts to common sorbents, such as activated carbon, clay, zeolite, and diatomite [69]. Graphene is primarily derived from single-layer graphite and has a lot of potential for environmental services. A 3-D carbon NM was formed by converting a 2-D NM into a 3-D microporous structure [70]. The 3-D carbon nanostructures are constructed using a range of fabrication procedures precisely described in the next section. The structure and interfacial interactions with encompassing bulk materials define the physicochemical characteristics of carbon nanostructures. Drugs with high water solubility get adsorbed in target tissues/cells in humans, animals, and plants as they are extremely persistent in the environment and stable under ordinary circumstances. Each year, thousands of tons of drug substances and pharmaceutical constituents are introduced into the environment, with excess medicines responsible for a major amount of this [71,72]. Additionally, they are re-converted to active components via metabolic processes, and pharmaceutical pollutants are particularly common in cosmopolitan sewage. Graphene-based NMs also treat wastewater because they have vital physicochemical characteristics, such as large surface area, facile functionalization, and hydrophobicity [72,73]. Graphene nanocomposites (NCs) also act as nano-sorbents for removing hazardous and noxious mixtures of numerous contaminants and catalytic decomposition of those pollutants using catalytic, visible light photocatalytic oxidation and reduction, and electrocatalytic processes. On the other hand, commercial production and usage are still major obstacles [74]. Nanoporous graphene sheets may filter and desalinate water by changing their pore size and pressure. However, their mechanical stability after increasing the pore number is the primary restriction [75]. Using the self-assembly fabrication technique, Yan et al. [76] fabricated N-doped sandwich shape graphene NCs for the deionization of electrodes. The formed heterocomposite delivered a specific large surface area, less electronic resistivity, and better adsorption ability with efficient, recyclable characteristics. They also represented that graphene sheets are

applicable as selective barriers for water penetrability. Graphene sheets are superoleophilic and superhydrophobic in nature and thus can be applied as an absorbent for numerous other NMs, signifying their extreme selective nature, appropriate recyclability, and substantial absorption abilities of even more the 90%. The aqueous elimination of hazardous dyes by graphene derived nano-adsorbents has several benefits over CNT-based NMs because single-layered graphene or single-layered CNT shown two basal planes reachable for pollutant adsorption [77]. Furthermore, graphene and its derivatives can be easily synthesized via chemical/mechanical exfoliation of graphite without employing complicated equipment. Notably, the obtained graphene derived NPs are free from residues of catalytic reactions, thus hindering the necessity for further purification processing. Mostly in the case of graphene oxide, the nano-sorbents provide a large number of O_2-bearing functionalities, hence prohibiting further acid treatments from promoting reactivity and hydrophilicity of the NM [78]. Favorably, their interaction, such as electrostatic π-π and hydrophobic contacts with a variety of organic and inorganic pollutants, represents the potential of graphene oxides for acting as a good nano-sorbent for polluted water and wastewater [79]. The science world is positive about carbon nanostructured materials attaining considerably better sustainable energy conversion and waste management.

Carbon and graphene quantum dots represent an interesting group of NMs with extensive applications among nano-carbon materials [80]. Xu et al. [81] discovered quantum-sized carbon dots in 2004 (a few months before graphene counterparts), and Sun et al. [82] gave them the popular moniker "CQDs" in 2006. However, their use as heterogeneous photocatalysts only began lately. CQDs are carbon-based 10-nanometer NPs with a flat or quasi-spherical form, sp^3 or sp^2 hybridized carbon atoms (i.e., diamond shape-like and graphene sheets like structure), composition-dependent fluorescence, and a variety of surface functional groups [83]. Graphene quantum dots (GQDs) primarily comprise a single graphene layer with a size not greater than 2 nm. Carbon-based nanodots, CQDs, graphene quantum dots GQDs, and carbon nitride dots are all these NMs that belong to the same carbon family [84]. These carbon-based nanostructures demonstrate intriguing involvement in non-biomedical regions, such as optoelectronic components and visible light photocatalysis, because of their eclectic properties, which include strongly size-dependent automated, electrochemical, and optical, as well as quantum size effects, easy surface modification, customizable composition, the ability to channel long-wavelength light, and ease of fabrication [85].

Furthermore, CQDs and GQDs are also promising candidates for biological and medical equipment, including therapeutics, bio-sensing, gene editing, and bio-imaging, owing to their advantages, which include nontoxicity, high photo-stability, remarkable electronic stability in vivo, biocompatibility, electro-chemiluminescence, non-linear optical feedback, intense and infinitely adaptable photoluminescence (PL) with the use of surface functional groups, and dot size, among other things [86,87]. Based on density functional theory (DFT), GQDs may be altered from deep UV to NIR; Chen et al. [88] demonstrated that by modulating the morphological properties, surface functional groups, particle size, edge configuration, defects in surface, and doping of heteroatom, results in the (near-infrared). Graphene (i.e., 0-D CQDs, 2-D graphene sheets), nano-diamonds and CNTs are the most well-known carbon-based NMs in NCs. GQDs might also self-assemble into honeycomb nanostructures or hollow microspheres [89]. In addition to having the potential to act as an alternative semiconductor, which has severe demerits of toxicity and high cost, carbon NPs could impact the quality of several nano/photocatalysts through energy band alignment, morphometric change, light adsorption augmentation, synergic coexistence, and charge transferal promotion, among other mechanisms [90]. Because of their high photon absorption, fully available surface, outstanding photo-stability, high miscibility, tunable band gap structure, and potential to fabricate heterostructures or hybrids with others, nanostructures have been widely used as efficient nano-photocatalysts for photocatalytic energy generation as well as in the visible light photocatalytic deterioration of pollutants. Figure 2 concisely represents the qualities of carbon-based materials and portrays their

potential as a future NMs for a broad range of implementations in the environmental remediation sector.

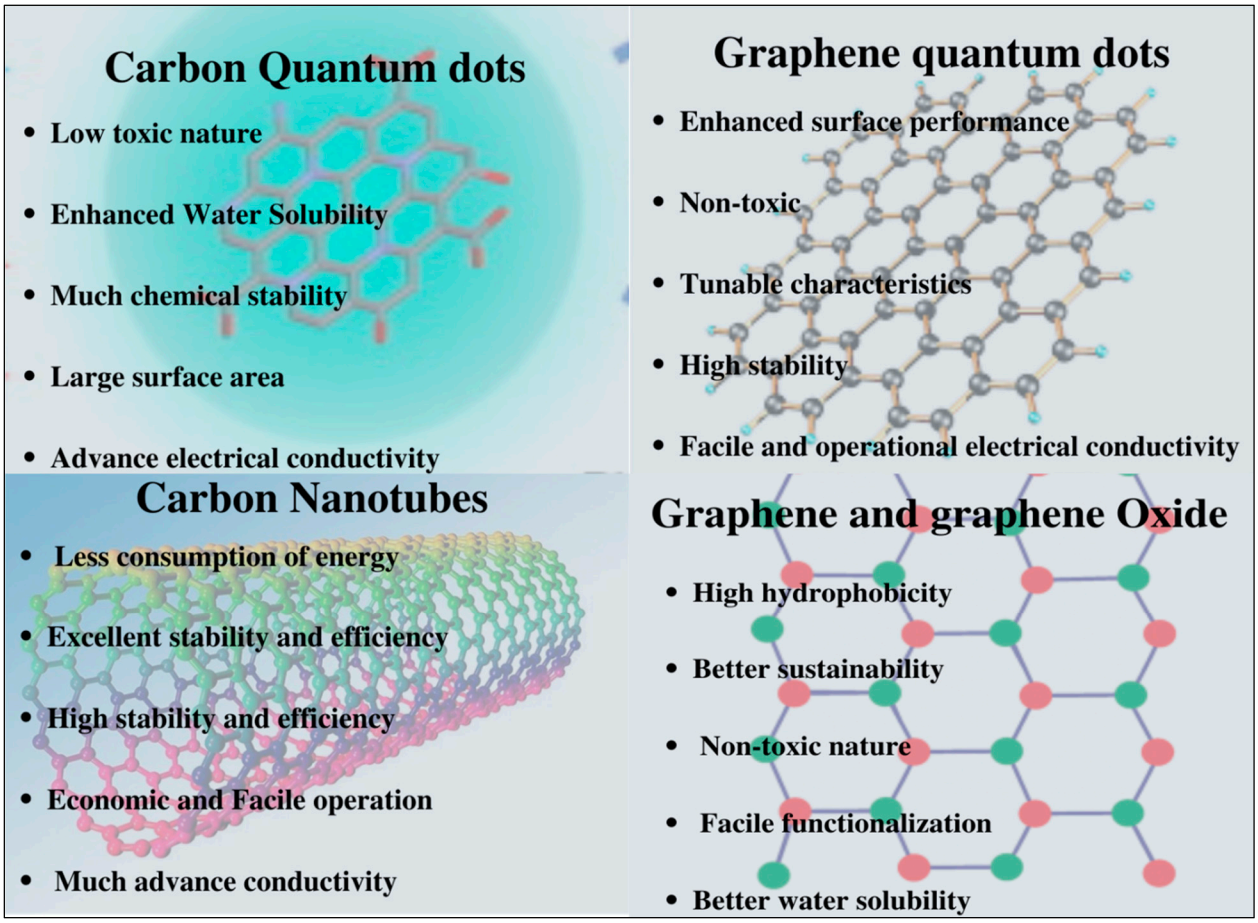

Figure 2. Various carbon-based NMs and their number of distinct advantages.

3. Fabrication of Carbon Nanoparticles

The introduction of next-generation nano-carbon composites, such as sophisticated components with enhanced performance and multifunctionality, has piqued attention [91]. Carbon-based precursors, such as graphene and CNTs, are critical in assessing the long-term viability of the technology. To date, carbon precursors, such as acetylene, methane, benzene, toluene, and xylene, have been employed to synthesize CNTs [92,93]. However, because of their dependence on natural resources, carbon-based precursors will suffer the problem of shortage in the future. Thus, a more economical, convenient, and eco-friendly way is needed to produce carbon-based NMs [94,95]. Inexhaustible and cost-effective, natural antecedents as a reservoir of hydrocarbons might be a green choice for large-scale manufacturing of NMs. As a carbon substrate for the manufacturing of CNTs, natural precursors represent an attractive option because of their low cost and lack of scarcity in the near future. Instead of depleting a natural resource, every manufacturing plant must use renewable feedstock to comply with the green chemistry idea [96]. In addition, the process must be achieved by incorporating as many of the feedstock's component atoms as feasible into the final product. Using natural carbon NM precursors has lately gained a lot of attention as a safe and ecologically friendly solution to a broad variety of applications. Massive amounts of carbon-based materials, such as CNTs and graphene, can already be manufactured using natural hydrocarbon antecedents and recyclable materials, proving that the themes of synthesis antecedents may be obtained in large numbers [97]. The combustion of plant-derived antecedents and residues, including textiles, seeds, bagasse, and hydrocarbons, has provided a variety of carbon products. According to studies on the

ultrastructure of plant parts and carbon formed by them, plant-derived precursors display some basic hydrocarbon components, such as skeletal structures. Natural precursors have lower market pricing than fossil, gaseous, and liquid hydrocarbons [98]. The 1-D and 2-D carbon structures represent the basic raw natural hydrocarbon components. These natural precursors provide an ecologically friendly way to manufacture CNT_S and graphene on a wide scale for diverse environmental applications.

3.1. Conventional Fabrication Techniques

Graphene and CNTs are generally produced by synthesizing fossil hydrocarbons, which are costly and difficult to acquire. A catalyst working on gaseous fossil species originating from the thermal decomposition of hydrocarbons is generally accountable for the formation of graphene and CNTs [99,100]. It has been possible to manufacture several kinds of CNTs, carbon nanofibers (CNFs), vapor produced carbon fibre, and other categories of carbon nanoscale materials using a variety of different processes, including, when it comes to synthesizing nano carbon-based substances, some of the most popular methods, i.e., laser ablation, arc discharge, and CVD (chemical vapor deposition) [101]. Heterogeneous CVD processes essentially comprise passing a gaseous or liquid flow having a specific proportion of a hydrocarbon, such as xylene (C_8H_{10}), benzene (C_6H_6), toluene (C_7H_8), acetylene (C_2H_2), methanol (CH_3OH), ethanol (C_2H_5OH), hexane (C_6H_{14}), methane (CH_4), and carbon monoxide (CO) over the nano surface of metal particles, such as Cu and Fe, Co, Ni), in the furnace. For the fabrication of graphene and CNTs, solid carbon sources, such as polyimide, polymethyl methacrylate (PMMA), and coal, have been employed. The majorities of liquid and gaseous fossil hydrocarbons are poisonous or explosive and harmful to the environment and human health [102,103]. Figure 3 depicts the various gaseous and liquid hydrocarbon fossils often utilized to synthesize carbon-based NMs at higher temperatures using various metals acting as catalysts. Various techniques used to fabricate carbon-based NMs are chemical oxidation, atmospheric plasma-based fabrication, hydrothermal carbonization, microwave aided fabrication, ultrasonic techniques, solvothermal methodology, thermolysis, laser ablation approach, and electrochemical approach [104,105]. Different synthesis procedures allow for fine-tuning carbon-based nanostructures size, component elements, and characteristics. A strong oxidant oxidizes a carbon precursor to carbon dots in chemical oxidation. Carbon dot fabrication on a wide scale is a rather simple technology [106]. Unfortunately, a fundamental drawback of this approach is the lack of uniformity in the size distribution of the resulting particles. Laser ablation is a simple and quick method to fabricate carbon NPs in which a laser is used to irradiate a carbon target [107,108]. However, this approach has large energy consumption and a poor quantum yield. It is also a costly technology that does not secure NPs size control. Hu et al. [109] investigated the influence of laser pulse width on carbon dot size and shape. They demonstrated that the pulse width had a significant impact on the nucleation and proliferation of fabricated particles. The effect of carbon NPs size and surface states on optical properties and photoluminescence has been studied. The size of the fabricated NPs may be determined by varying the proportion of HNO_3 used for oxidative refluxing, and selective reduction with $NaBH_4$ changes the surface states. Electrochemical oxidation synthesizes carbon NPs with high purity and yield and adjustable shape and size. However, due to the technique's extensive processing processes, it is only of limited utility. Graphite rod, carbon paste, and carbon fibre are the electrodes utilized [110]. Liu et al. [111] described an electrochemical synthesis that employs graphite as the working electrode, platinum foil as the counter electrode, and Ag/AgCl as the reference electrode. They created carbon dots with an average diameter of 0.2–4.0 nm that they utilized to detect Fe^{3+} ions in drinking water. Ultrasonic energy has been frequently employed for carbon dot fabrication because of the process's simplicity, cost-effective, and absence of secondary contamination. Wu et al. [112] used an ultrasonic approach to fabricate amine-decorated carbon dots from graphite rods. The fabricated carbon dots were useful for detecting cobalt (II) ions in actual samples and sensing nucleic acids in living cells. Carbon dots were

fabricated from urea, citric acid, and polyethylene glycol via ultrasonic processing as a lubricant [113–115]. The carbon core and tiny size, which provide a rolling effect, were associated with the lubricating action. The microwave approach, which requires a minimal reaction time, provides a simple and cost-effective synthesis. This simple process can produce size-controlled particles with a high yield, but it requires a lot of energy. In addition, the approach is limited by unpredictable reaction parameters [116,117]. Microwaves were used to carbonize a combination of citric acid and *Citrus japonica* to synthesize biocompatible luminous carbon dots for biological uses [118]. For the synthesis of simple, doped, and supported carbon-based NPs, the solvothermal approach, particularly the hydrothermal method, is the most widely used methodology [118–121]. It comprises a chemical reaction in a solvent such as water in a sealed pressure vessel. Environmental friendliness, very moderate working conditions, a one-step synthesis approach, and excellent dispersion in solution are all advantages of this technology. As a result, a broad range of precursors has been employed to synthesize carbon-based NMs using the hydrothermal approach, including aloe, papaya, cornstalk, water hyacinth, apple juice, and milk. It is an effective strategy for cost-effectiveness and convenience of use [122–126]. The thermal breakdown is an affordable solvent-free fabrication method, although the resulting particles lack a uniform distribution of NPs [127]. Despite significant advances in the sector of carbon-based NMs fabrication, the employment of demanding reaction conditions, hazardous precursors, and post-synthetic processes for surface passivation generally complicates the process and prevents their widespread adoption. The majorities of the papers have clear drawbacks, such as high-cost equipment, the use of corrosive chemicals, and non-homogeneity of the resultant NPs, and hence are not cost-effective. Various research groups have experimented with easier and lower-cost synthesis strategies and the use of environmentally acceptable precursors [106,128,129]. Many review articles have been published imparting the information regarding the use of hydrocarbons for the fabrication of carbon NMs, but only a few of them have discussed the utilization of waste products as a precursor [128,129]. Thus, there is an utter demand to the scientific community for green, economic, as well as renewable synthesis fabrication of these NPs for environmental applications.

3.2. "Green" Synthesis of Carbon-Based Nanomaterials

Naturally occurring plant hydrocarbon precursor and organic waste are renewable, low-cost, and widely available sources of hydrocarbon for the fabrication of various carbon nanostructures [130]. Thus, we can synthesize the carbon-based NMs on a large scale by utilizing these natural waste products [131]. As a source of carbon for high-quality CNT and graphene, renewable antecedents and waste products may provide a number of benefits [132]. These precursors generate a sustainable amount, are safe for the environment, and are cost-effective. In addition, a variety of usable energy and energy activities could benefit from the usage of high-quality carbon-based nanostructures naturally derived from antecedents and waste products [133]. The various types of natural precursors, edible food, and scrap material employed to fabricate numerous new innovative carbon nanostructures are depicted in Figure 4. For the green production of carbon-based NPs, diverse kinds of plant are employed as renewable carbon feedstocks [134]. The leaves, flowers, and roots are the most widely utilized plant. Shells, bark, stem, and peels are examples of plant biomass [135,136]. Pre-processing is necessary to reduce particle size and remove excess water from these feed sources [137]. Drying the feedstock under full sun saves energy in comparison to more traditional methods of dehydration. For hydrothermal synthesis, fruit juice is advantageous since it provides a "ready-to-use" solution, avoiding the need to revive dried plant components. However, this advantage comes from sacrificing the diversity of carbon seen in dry feedstocks. For example, Lotfy and colleagues generated citric acid from *Aspergillus niger* with a 90% yield using beet and maize steep liquors and salts as feedstocks [138]. There is a lot of citric acid in citrus fruits, which account for up to 8% of the dried fruit mass. Researchers have used L-glutathione and celery leaves to make

carbon NPs via hydrothermal synthesis as part of hybrid green syntheses that combine renewable raw materials with renewable refined products.

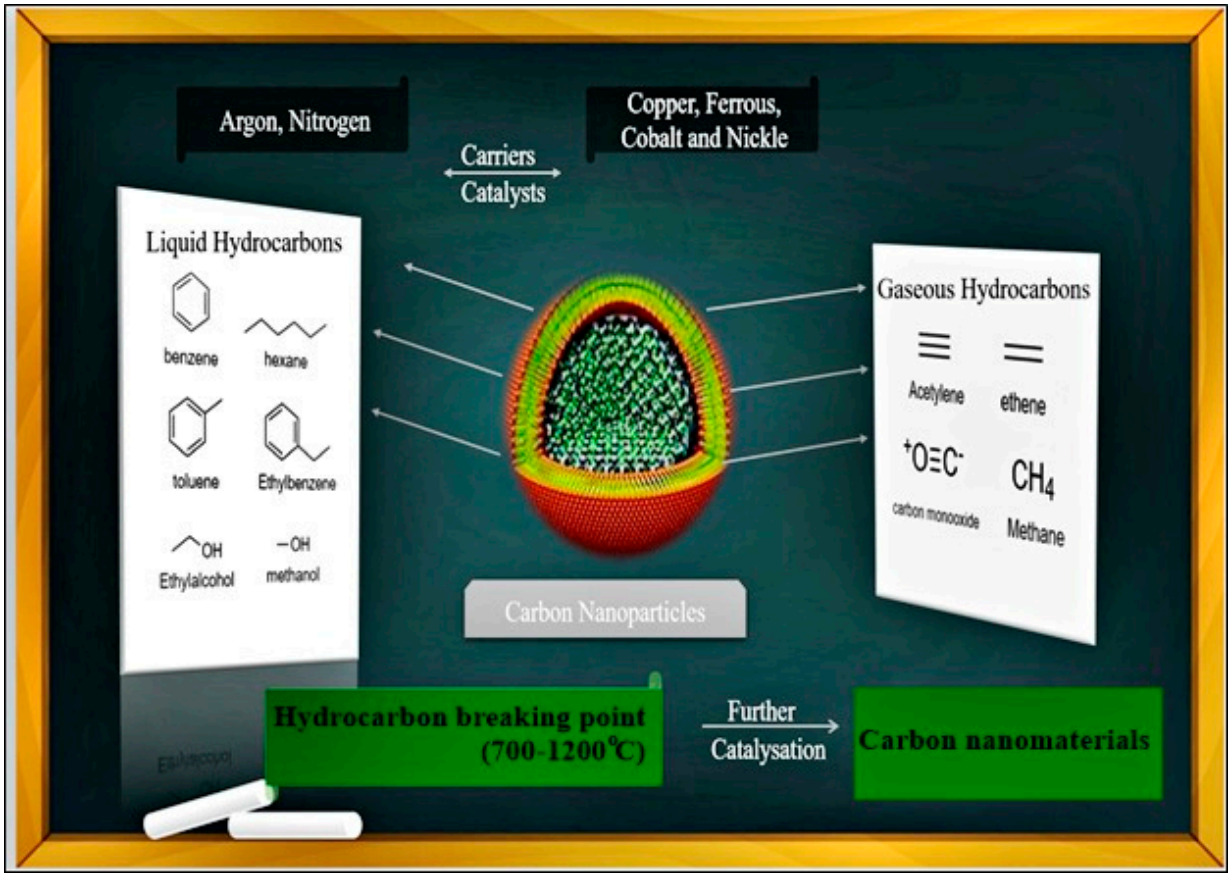

Figure 3. Various liquid and gaseous hydrocarbon fossils utilized for the fabrication of carbon-based NMs at higher temperatures using various metals acting as catalyst.

Bio-oils also represent a potential candidate for the fabrication of CNTs due to their cost-effectiveness and easy availability, thus making them an excellent green antecedent for CNT production. A major component of eucalyptus oil has the chemical formula $C_{10}H_{18}O$, which comprises carbon, hydrogen, and a small proportion of oxygen. For instance, under atmospheric pressure, Ghosh et al. [98] employed eucalyptus oil as a catalyst and Fe/Co coated on zeolite as the catalyst support to establish a straightforward, and cost-effective technique for the production of single-walled carbon nanotubes (SWCNTs) with low energy consumption. This fabrication approach does not require any prior treatment of the catalyst precursor to manufacture an active catalyst precursor. SEM (Figure 5a) and HRTEM images (Figure 5b,c) of the as-grown SWCNTs are represented in Figure 5, demonstrating the development of thick CNTs on the whole surface of the zeolite particles. The SWCNTs formed are in bundles, as per HRTEM studies. Kumar et al. [139] employed sunflower oil to synthesize aligned bamboo-shaped nitrogen-doped carbon nanotubes (N-CNTs). SEM and TEM results (Figure 5d,e) revealed that fabricated nanotubes lie parallel to the quartz tube's walls and have a consistent length of roughly 25 m. The N-CNTs in the form of bamboo were constructed from several segments with declining segment spacing and approximately equivalent numbers of layers, resulting in a bamboo-shaped structure. A cap of Fe catalyst particles is placed on top of the N-CNTs, and seven graphitic layers are used to recreate the hollow segments of the bamboo structures. In addition to the obvious natural hydrocarbon precursors, graphene and carbon nanotubes have indeed been derived from many diverse other eatable foodstuffs, such as honey and sugar, and fats and dairy products, such as butter, milk, and cheese, for graphene synthesis.

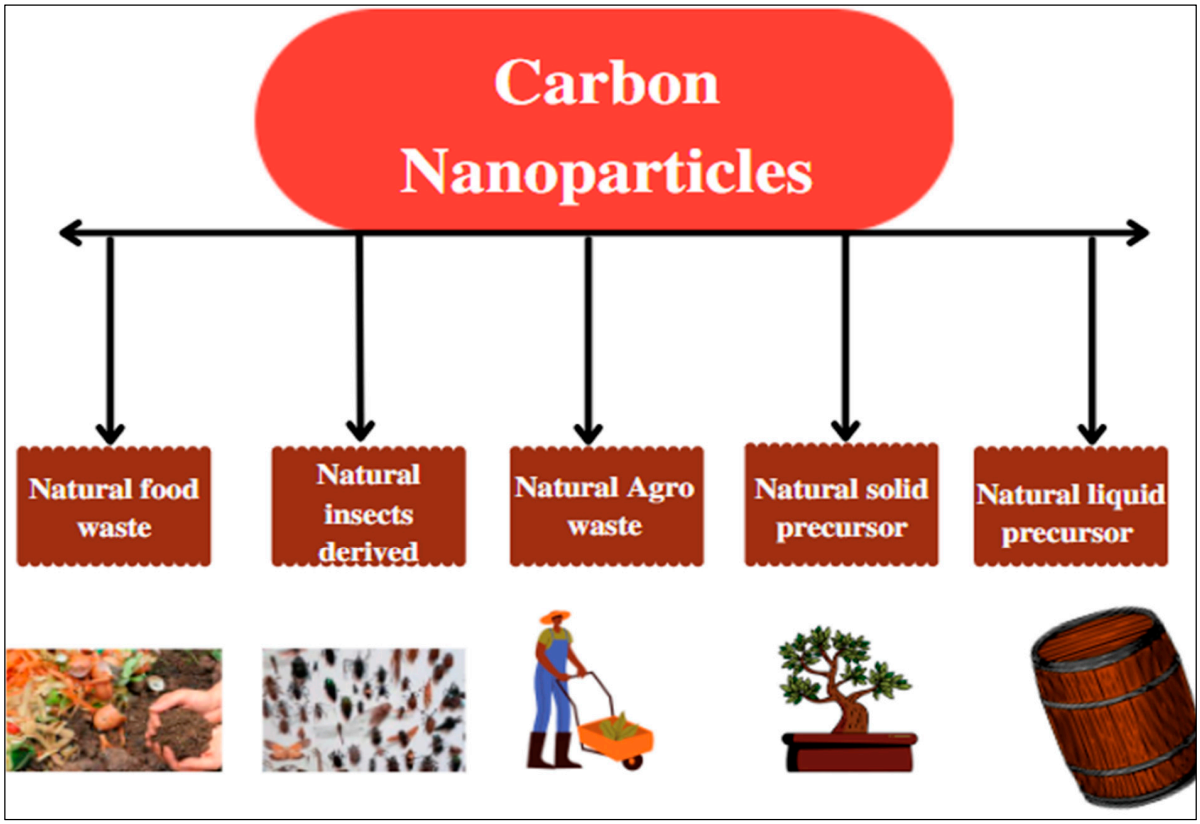

Figure 4. The various types of natural precursors, edible food, and scrap material employed for the fabrication of numerous new innovative carbon nanostructures.

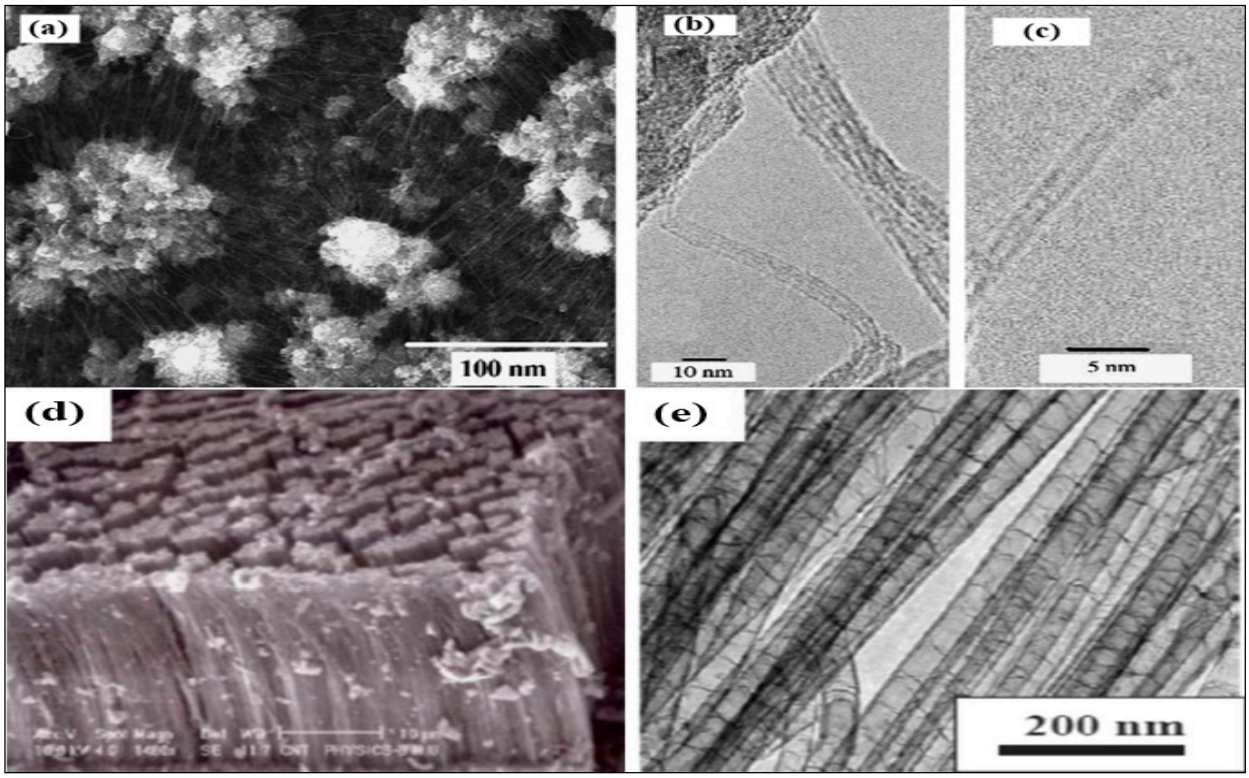

Figure 5. (**a**) SEM, (**b**,**c**) HRTEM images of SWCNTs grew in the zeolite matrix, Nitrogen doped CNTs using sunflower oil (**d**) SEM image and (**e**) TEM image (Reprinted with permission from [98] Elsevier, License No. 5399121364489).

Seo et al. [140] reported a unique plasma approach for fabricating nano-graphene sheets employing five distinct eatable foodstuffs, including butter, honey, milk, cheese, and sugar, in various physical states. This plasma-enabled, low-temperature (450 °C) technique uses renewable natural resources and does not require any catalysts or hazardous precursors. The main advantage of this strategy is that it works for a variety of precursors, including honey, sugar, and milk. Figure 6 depicts the characteristics of several precursors in various stages. The authors showed how honey, butter, table sugar, and condensed milk might be converted into nano-graphene sheets without other catalysts or external heating when treated with hydrogen and argon plasma. Fabricated nano-graphene sheets are employed for bio-sensing applications. A convenient method for the fabrication of highly crystalline carbon dots has been proposed through a plasma-induced methodology. Wang et al. [141] reported a plasma-induced technique for synthesizing carbon dots utilizing inexpensive and natural chicken eggs as the precursor, and this approach may be utilized to make carbon dots from a variety of carbon sources. Thus, the prospects of these carbon dots as fluorescent inks for multicolor patterning utilizing inkjet and silk-screen printing have been expanded.

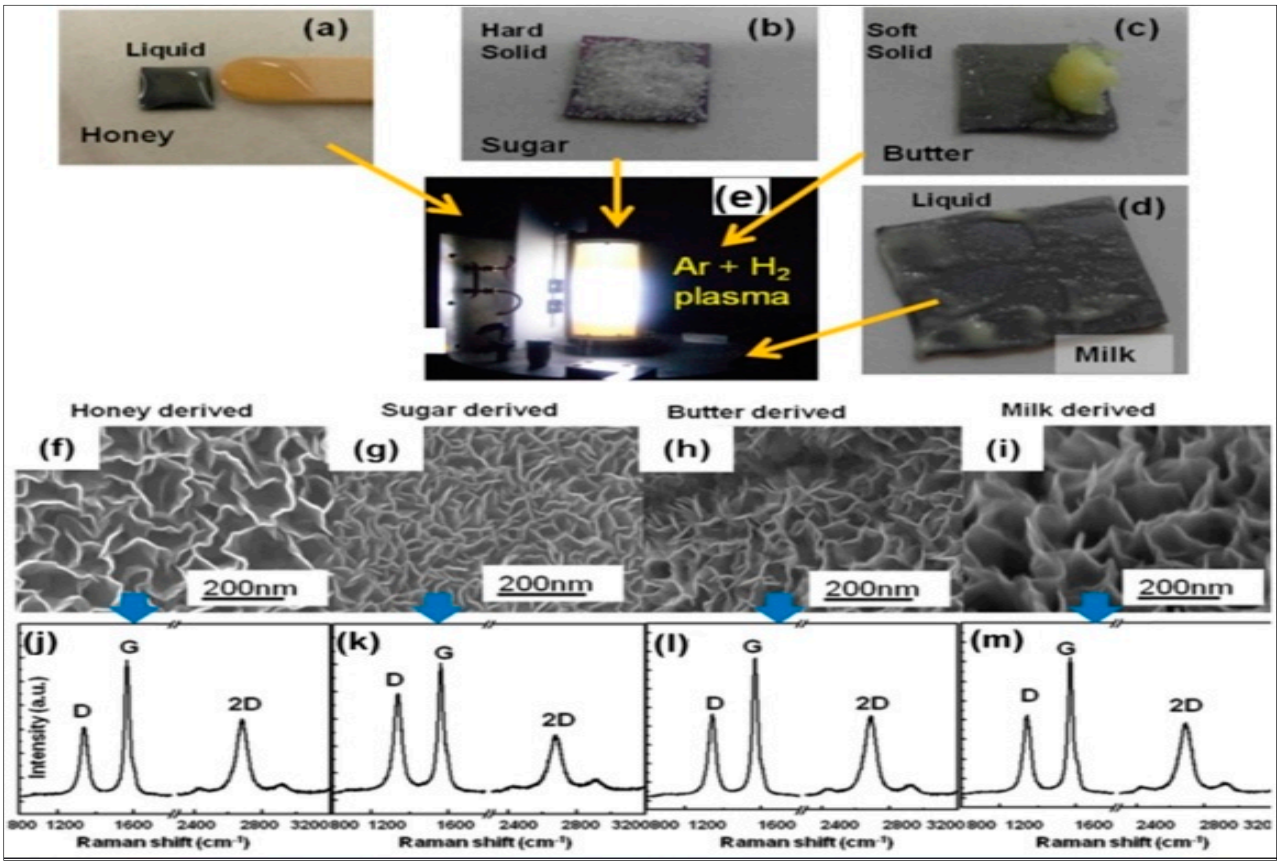

Figure 6. Synthesis and characterization of graphene nano-sheets via plasma-based technique with natural precursors. Images of natural antecedents in various stages placed on pure SiO_2 substrates, and (**e**) the plasma used to make vertical graphene (**a**–**d**). SEM and Raman spectra of fabricated Graphene nano-sheets fabricated using (**f**,**j**) honey, (**g**,**k**) sugar, (**h**,**l**) butter, and (**i**,**m**) milk. (Reprinted with permission from [140] John Wiley and Sons, License No. 5399130576609).

A novel NCs system based on CNTs, graphene, and its derivatives is evolving for use in multifarious applications in biology, chemistry, medicine, and physics. Recently, graphene and carbon nanotube production methods, such as spray pyrolysis and CVD, have made significant strides thanks to advances in carbon nanostructure technology. However, carbon precursors derived from fossil fuels, such as acetylene, benzene, methane,

and other hydrocarbons, which are frequently used in the manufacturing of carbon-based nanostructures, have a limited stock, damage the environment, and will be unreachable in the foreseeable future due to a lack of available resources. It may be appropriate to use natural precursors, eatable products, and residual carbon-containing products as a benchmark in this situation. It is anticipated that the use of these resources as carbon source precursors would cut the cost and use of scarce fossil fuels and aid us in treating our environment with more sensitivity. The production of eucalyptus oil, turpentine oil, palm oil, biodiesel, sunflower seed oil, neem oil, castor oil, and other natural precursors may be done effectively, in an ecologically acceptable way, and in an environmentally friendly setting. In addition, there are a plethora of massive carbon-containing waste materials strewn across the environment. The chances are that they have been discarded, and so they are contaminating the environment with little to no chance. These materials can be used to make a variety of carbon nanostructures with ease (Figure 7). From surface properties to large-scale manufacturing, natural waste products from the creation of graphene and carbon nanotubes will continue to make significant contributions to the forefront of nanotechnology and related bulk commodities for many generations to follow.

Figure 7. For the manufacture of various novel revolutionary carbon nanostructures, various natural precursors, widely used.

4. Environmental Applications

Unique physicochemical features of NPs have made them an attractive candidate for use in bioremediation and improving performance in the renewable energy industry. NPs are present in nature, and some of them have been discovered to help the environment [142]. For more than a decade, environmental remediation utilizing NPs, also known as nano-remediation, has been effectively employed to clean or decontaminate the air, water, and soil [143]. Nano-remediation is among the most efficient alternatives since it provides in-situ treatment, eliminating the need to pump groundwater out for diagnosis and excavating to reach the desired region. The NPs are introduced into the appropriate site and carried along with the groundwater flow, disinfecting the water by immobilizing pollutants. Redox reactions represent the general process involved in decontamination. Surface water is treated with NPs for disinfection, purification, and desalination [144]. Heavy metals, viruses, and organic pollutants are the most likely contaminants. It is effective, obviating the requirement for chemicals that might result in secondary reaction products. NPs are primarily used to remediate sewage water and the resulting sludge. NPs replace traditional

chemicals because they are less expensive, more efficient, and need less treatment volume. Nano-filtration is a mainly new membrane filtration approach for water purification that has remarkable use in the food and dairy sectors [145]. The utilization of NPs for renewable energy is the subject of much investigation. Solar cells with higher light and UV absorption and low reflection coatings have increased their efficiency significantly. Self-cleaning solar cells have been developed thanks to the hydrophobic features of certain NPs. Certain NPs with high thermal conductivity and heat absorption capacity cover boilers and solar concentrators to increase their thermal efficiency [146].

4.1. Water Treatment Using Carbon-Based Nanoparticles

Photocatalysis refers to the use of an appropriate catalyst to speed up photoreactions. Hydroxide free radicals are used in the majority of photocatalyzed processes. The water electrolysis process, made feasible by titanium dioxide, can be identified as the progenitor of the photocatalysis reaction. An important challenge was how to remove various pollutants from wastewater by using photocatalytic and adsorption techniques in combination to remove a broad spectrum of contaminants. Photosynthetic photocatalysis assists in the degradation of organic pollutants, which may then be removed through adsorption. Carbon nanotubes may be employed as photocatalyst carriers because of their porous structure, unique electrical structure, amazing chemical stability, strong absorption ability, and nanoscale hollow tube characteristic. Over the last few years, the remediation of industrial wastewaters from the urban and industrial sectors has garnered considerable attention. With a rapidly rising population, maintaining a consistent, clean water supply has become progressively difficult with a rapidly rising population, and severe drought has become common [147]. The detection of heavy metals in the environment, polycyclic aromatic hydrocarbons, total suspended solids, as well as organic and inorganic wastes would negatively impact the health of humans. Human care and development are inextricably related to basic sanitation and water availability. As a result, it has become necessary to treat wastewater streams to recirculate the cleaned water [148]. Several treatment methods employed include biological, chemical, and physical processes. Carbon-based NMs have also made their way into the wastewater treatment process, where they may be used as adsorbents to remove contaminants. As a result of their large surface areas and availability of surface adsorption sites, bi-functional CNTs have indeed been extensively investigated. It is being explored if functionalized single-walled nanotubes (also known as SWCNTs) and multi-walled nanotubes (also known as MWCNTs) can adsorb heavy metal contaminants, such as arsenic and chromium [149]. Ahamad et al. [150] prepared NH_2-MWCNTs@Fe_3O_4 to eliminate the toxic dye methylene blue (MB) from water. MB dye concentration, pH, temperature, and contact duration were examined and optimized as adsorption factors. The Langmuir isotherm equation determined a maximum adsorption capacity of 178.5 mg g^{-1}, greater than other adsorbents employed for MB adsorption. The recycling analysis revealed that NH_2-MWCNTs@Fe_3O_4 might be utilized for several adsorption cycles without losing significant adsorption capability. All of the results demonstrated that NH_2-MWCNTs@Fe_3O_4 might be an effective, readily separable, and reusable adsorbent for the adsorptive removal of MB dye from polluted water. Zhang et al. [151] described a facile and economic hydrothermal technique to fabricate TiO_2 layers coating on CNTs NC. The TiO_2 NPs were found exceedingly consistent, and the NCs' layer thickness was adjusted. Meanwhile, MWCNTs operated as an electron transfer channel, thus enhancing photocatalytic efficacy substantially. To boost the photocatalytic effectiveness, they discovered that the shallow TiO_2 coating layer provided a quick way for electron transfer and was more efficient at separating carriers. The photo-oxidation and photo-reduction sensitivity of TiO_2 NPs were studied concerning the depth of the TiO_2 coating layer using photocatalytic dye degradation. Even under the best conditions, one-dimensional TiO_2@MWCNTs has a higher photocatalytic performance than the conventional anatase TiO_2 and P25. Saharan et al. [152] fabricated Sn doped MnO_2/CNTs via the co-precipitation technique. Fabricated NM was utilized to eliminate dyes via adsorption and for the electrochemical sensing of

thiourea (Figure 8a). The results revealed that the fabricated NC showed 95% of adsorption within 30 min and recovered successfully. Sn doped MnO_2/CNTs exhibited exceptional activity in terms of sensitivity also. Graphene has taken on a new role in wastewater remediation due to its unique physicochemical and surface features. Because they are 2-D NMs with a single-atom graphite layer, graphene oxides and functionalized graphene have been highly sought after for their ability to cleanse available polluted stream flows, sequester heavy metal ions, rare-earth metals, and organic molecules. Graphene and its related materials are also being researched as possible photocatalysts because of their capacity to break down pollutants. For example, graphene possesses a better UV–visible light transmittance than other carbon compounds, superior electrical and thermal conductivities, and greater corrosion resistance than other carbon compounds. To reduce Cr(VI) under visible, UV, and NIR light irradiation, Wu et al. [153] produced a variety of hybrid photocatalysts with various decreased graphene weight ratios and tested their photocatalytic efficiency. The CuS/RGO demonstrates high optical absorption and catalytic performance under full sunlight irradiation because of its synergistic influence. One weight percent of RGO total immersion in the hybrid photocatalysts may reduce Cr(VI) by 90% under total UV-Vis-NIR light irradiation. CuS and RGO's outstanding activity may be ascribed to robust absorption across the entire solar spectrum and effective charge segregation and transfer due to their similar energy levels and excellent interfacial contact. Photogenerated electrons have been found to influence the catalytic process. While CuS absorbs photon energy (Figure 8b), it is driven by photons to the conduction band (CB), resulting in electron-hole pairs (EHPs). Electrons and holes migrated to the photocatalysts surfaces to complete the redox reactions. The photocatalytic reduced Cr(VI) process may reduce Cr(VI) to Cr(III) because the Cr(VI)/Cr(III) potential (0.51 V vs. NHE) is more positive than the CuS CB (-0.38 V against. NHE) and work function of RGO (-0.08 V vs. NHE). Pure CuS has minimal photocatalytic activity because the photo-induced charge carriers are recombined in the bulk and surface of the material. As a result, RGO served as an effective electron acceptor to collect photo-induced electrons, considerably increasing separation efficiency and reducing charge carrier recombination, thereby boosting photocatalytic performance. New UV-Vis-NIR light photocatalyst technologies may be developed based on this study, which might be used to clean the environment and convert energy.

The use of graphene oxide to improve photocatalytic efficiency has gotten a lot of interest. Many contaminants have been effectively eliminated using graphene and its derivatives, including chromium, formaldehyde, bisphenol A, and tetracycline. Reduced graphene oxide/titanate nanotube hybrid NCs with different loading of reduced graphene were fabricated via a simple hydrothermal technique by Nguyen et al. [154]. Hybrid structures containing rGO have significant application potential because of the synergetic effect produced by the enhanced adsorption of the cationic dye methylene blue and the isolation of photogenerated electron–hole pairs. The photodegradation of MB by reduced graphene oxide/titanate nanotube (rGO/TNT) composites was significantly improved compared to other catalysts such as TiO_2 when exposed to UV and visible light. When evaluated with other artificial catalysts, the rGO/TNT composite containing 3 wt% rGO had the greatest decolorization and mineralization activity compared to the other catalysts; achieved about 100% decolorization and 77.4% mineralization after one hour of UV irradiation. However, 95% decolorization and 78.8% mineralization were achieved after three hours of visible light irradiation. P25 improved the removal of anionic dye MB compared to rGO/TNT composites. However, the 3% rGO/TNT composite exhibited the significant photocatalytic performance among the produced NMs studied. Based on these results, it is hypothesized that hybrid rGO/TNT composites may be employed as adsorbents and photocatalysts to efficiently and completely remove hazardous dyes from water prior to recycling. Other nano-carbon molecules being investigated in this sector include carbon quantum dots, fullerenes, and similar chemicals. Zhang et al. [155] used a hydrothermal process to fabricate Fe_2O_3/CQDs NCs that were effective semiconductor photocatalysts for the photo-degradation of toxic fumes such as methanol or benzene under visible-light

conditions. The pathway for Fe_2O_3/CQDs NC with cubic morphological features of magnetic architecture and their photochemical use is depicted in Figure 9a–c. Because of the unique properties of CQDs, magnetic nano-hybrids can combine magnetic properties with fluorescence on one substrate. Because of the high electron storage capacity of CQD (shown in Figure 9d), electrons stimulated by photons emitted from Fe_2O_3 NPs may move freely across the CQD conducting system. An increase in the number of active oxygen radicals capable of removing dangerous gases may be achieved by the interaction of the adsorbent reductants/oxidants with the electron-hole pairs.

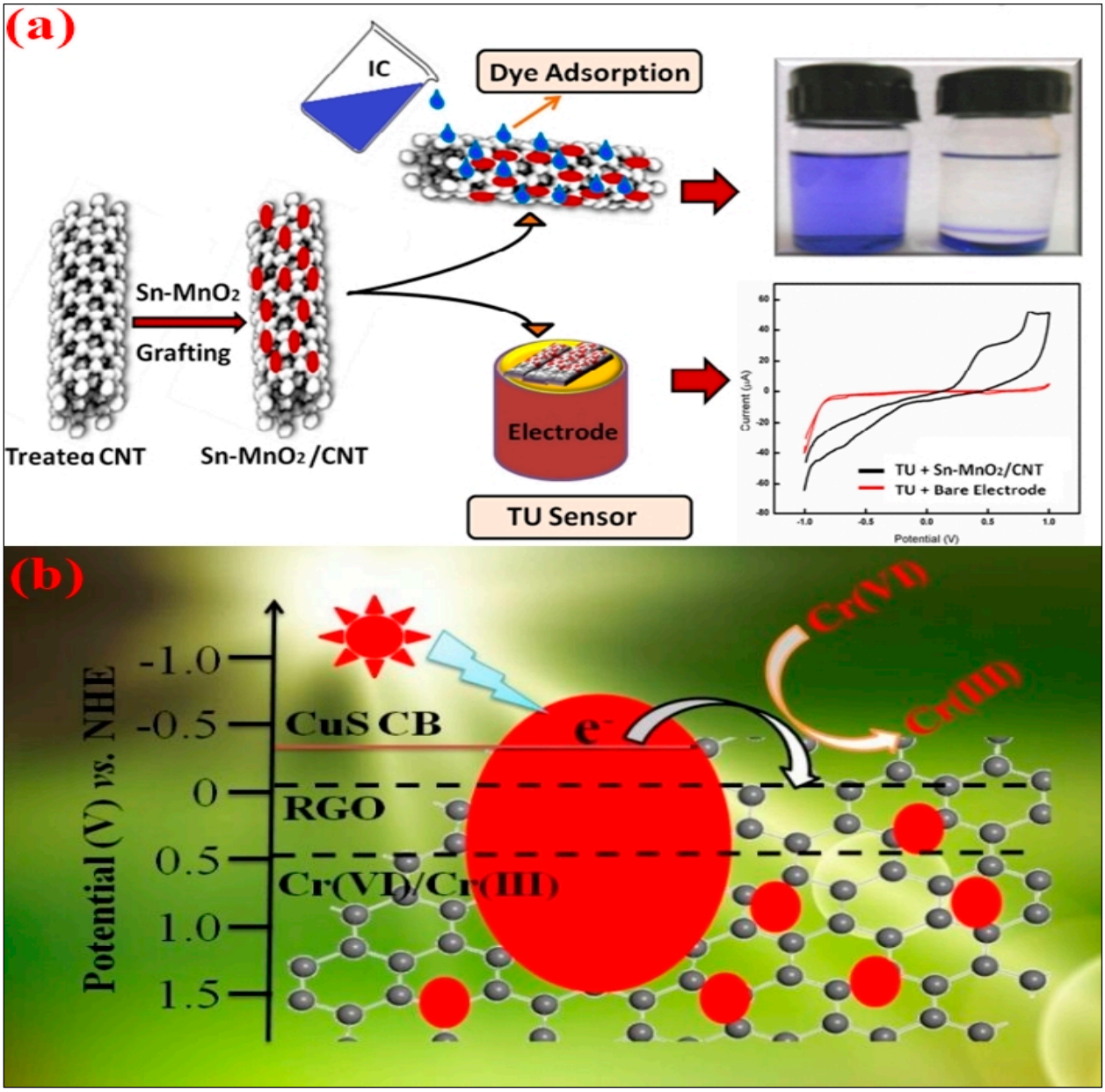

Figure 8. (**a**) Fabricated Sn doped MnO_2/CNT NM utilized for elimination of dyes via adsorption and also for electro-chemical sensing of thiourea (Reprinted with permission from [152] Elsevier, License No. 5399130850139), (**b**) photocatalytic mechanism of CuS/RGO for chromium photo-reduction (Reprinted with permission from [153] Elsevier, License No. 5399131060070).

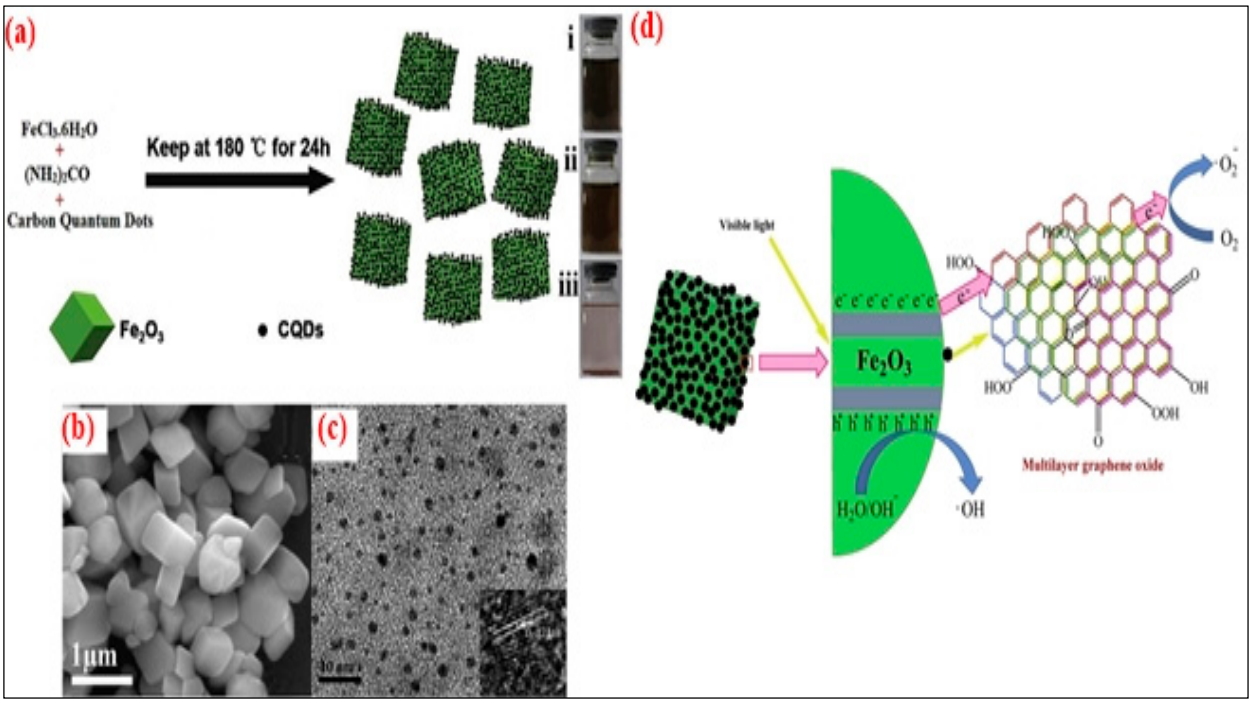

Figure 9. (**a**) Hydrothermal synthesis of Fe_2O_3/CQDs NCs, which photographs demonstrate; (i) aqueous dispersion of CQDs, (ii) solution containing CQDs, with precursors and (iii) final nano-composite, (**b**) SEM image of Fe_2O_3/CQDs, (**c**) HRTEM images of Fe_2O_3/CQDs NC, (**d**) schematic representation of interactions between CQDs and Fe_2O_3 NC indicating the exceptional photocatalytic performance under visible light. (Reprinted with permission from [155] Royal Society of Chemistry, License No. 600097123).

4.2. Carbon Nanomaterials for Hydrogen Evolution Reaction

As a dopant in carbon, hetero-atoms (e.g., B, P, N, S, or others) can change carbon's physical and chemical characteristics to acquire more reactive sites. More crucially, this technique can synthesize carbon-based NMs that have a higher capability to adsorb the atomic/molecular species involved in catalytic processes while maintaining their conductive characteristics [156]. These heteroatom-doped structures might open the opportunities for the sustainable development of cost-effective metal-free catalysts with high activity and long spans. The difference in electronegativity and size of hetero-atoms and carbon has been reported to polarize nearby carbon atoms to assist the oxygen reduction reaction, which might be used in the hydrogen evolution [157]. The first design and synthesis of a 3D N-graphene-C_3N_4 hybrid film with a microstructure equivalent to van der Waals heterostructures were reported by Duan et al. [158]. A significant increase in catalytic activity was noticed in the novel material, making it a strong candidate for the next generations of HER catalysts (Figure 10a). It has also been discovered that superior structural characteristics of electrocatalysts, such as the richness of bare active sites, symbiotic pairing among porous carbon nitride (PCN) nano-layers and graphene sheets, hierarchical porous structure, and N-doping alteration graphene functionality, are associated with increased performance. Because of the packing of C_3N_4 within graphene sheets, the resulting catalyst displayed outstanding endurance over a long period when subjected to acidic conditions during cycling tests. Furthermore, this material was created using a straightforward approach that used low-cost precursors. As a result, it may be utilized to create a range of graphene-based 3D catalysts for an array of applicants, spanning hetero-catalysis, solar cells, and fuel cells, among others. Zhou et al. [157] reported that N-doped carbon-coated Co nanorod supported on a Ti, i.e., Co@NC/Ti, was fabricated by a two-step approach. Electrochemical experiments demonstrated that the electrocatalysts had a high HER activity, with an onset potential of −56 mV (vs. RHE), and a substantial current density (10 mA cm^{-2}

at −106 mV), a modest Tafel slope of 78.2 mV dec^{-1}, and good electrochemical durability. The findings might lead to a new technique for designing and constructing efficient HER catalysts using earth-abundant and low-cost components. Liu et al. [159] described that the fabrication of carbon nano-dots extracted from rapeseed flower bee pollens was utilized to combine with ultrathin gC_3N_4 nano-sheets in a hydrothermal technique to form 2-D/0-D type photocatalysts. CQDs efficiently enlarged visible light absorption zones by photosensitization and suppressed photo-induced carrier recombination. According to electron paramagnetic resonance technology, fluorescence spectroscopy, and photo-electrochemical studies, CQDs act as electron transfer mediation to enhance charge separation and lengthen the lifespan of photo-induced carriers. The best H_2 evolution of the UCN/CQDs-0.2% composite is 88.1 mol/h; the UCN/CQDs composites had a significant photocatalytic efficacy for H_2 release when exposed to visible light. Figure 10b represents a plausible mechanism for improved photocatalytic performance in UCN/CQDs composites. To begin with, CQDs acted as an electron acceptor, allowing photo-induced electrons generated from UCN under visible light to easily shuttle to the conducting band of CQDs, thereby delaying recombination and extending the lifespan of electron-hole pairs. Second, like organic dyes, π- conjugations CQDs were utilized as a photosensitizer to sensitize UCN and donate electrons to its conduction band, resulting in a longer visible light response area for photocatalytic H_2 release. Finally, because of the up-conversion photoluminescence capabilities of CQDs, they may absorb longer wavelength visible light and subsequently emit shorter-wavelength light, causing UCN to create additional charge carriers. However, because the yield of photocatalytic hydrogen generation matches the PL results, the photogenerated charge-separation efficacy is the most important element in the photocatalytic performance of UCN/CQDs composites. Therefore, the limitation of quick charge carrier recombination in CN photocatalysts has been effectively controlled by creating 2-D/0-D heterostructures, resulting in improved photocatalytic effectiveness. Zhang et al. [160] reported an in-situ hydrothermal technique to accomplish a facile and green one-pot fabrication of titanate nanotube/graphene NCs. This ecologically friendly approach involves the direct development of well-defined TNT (titanate nanotube) uniformly dispersed on GR (graphene) substrates. Their photocatalytic H_2 evolution capacity was greatly enhanced by adding GR to TNTs. An array of energy and environmental issues might be addressed by these TNT/GR NCs, which have unique 2-D morphological features and a one-pot green hydrothermal method. To better understand the photocatalytic mechanism of the hydrogen evolution reaction from CH_3OH aqueous solution, Figure 10c depicts a possible reaction mechanism. After being irradiated by a Xe-lamp, electrons in the VB of TNT were excited to the CB of TNT, which left only holes in the VB, and the high energy electrons in the CB of TNT moved effectively through the interfacial contact between TNT and the GR sheet in order to reduce H or directly reduce water/proton to form H_2. Meanwhile, methanol, the sacrificial agent, scavenged the photo-induced holes in TNT's VB, limiting the recombination of charge carriers. It is important to note that when the loading percentage of GR surpasses 1%, black GR sheets restrict Xe-lamp illumination through the depths of the reaction solution and impede electron production from the interior of TNT/GR catalysts. A significant number of GR sheets also prohibited the expendable agents from coming into touch with the TNTs, which resulted in a decreased rate of H_2 formation. Furthermore, the H_2 evolution rate enhancement attained by combining TNT and GR is substantially greater than that investigated by Zhang et al., who fabricated TNP/GR NCs employing a one-pot hydrothermal approach with sacrificial agents Na_2S and Na_2SO_3. This is likely because, due to its 2-D p-conjugation structure, good electron conductivity, and the large contact area between TiO_2 and GR, GR acts as an electron-transfer channel and acceptor, extending the lifespan of charge carriers.

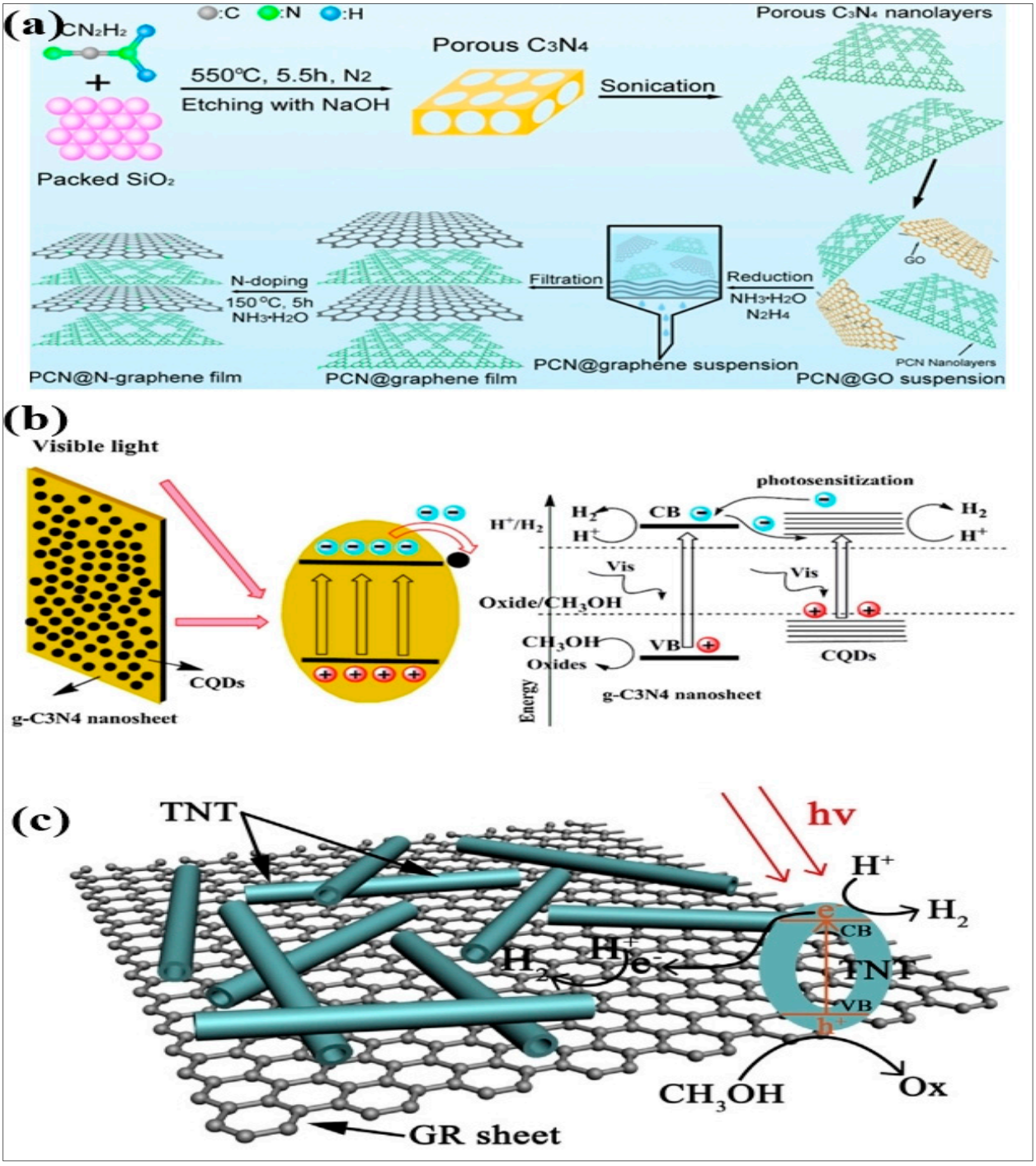

Figure 10. (**a**) Schematic representation for synthesis of PCN@N-graphene film, (Reprinted [158] copyright 2015 American Chemical Society) (**b**) graphical presentation of the photocatalytic mechanism of UCN/CQDs photocatalyst under visible light, (Reprinted with permission from [159] Elsevier, Li-cense No. 5402970976855) (**c**) charge transfer mechanism in TNT/GR photocatalyst under Xe-lamp. (Reprinted with permission from [160] Elsevier, License No. 5400000373804).

4.3. Carbon Nanomaterials for Gas Sensing

Technologies for identifying volatile organic compounds (VOCs) accurately and efficiently in fields, such as environmental gas monitoring, non-invasive medical diagnostics, and point-of-care activities, seem to be a promising direction in the development of future technologies. For one reason, VOCs are produced by diverse human activities, such as fuel burning, car exhaust emissions, and interior decor, resulting in the development of fine

particulate matter and ozone (O_3), causing major environmental issues including pollution and chemical smog [161]. On the other hand, the majorities of VOCs have a nasty odour and are poisonous, neurotoxic, mutagenic, and carcinogenic. Moreover, even at low concentrations, long-term exposure to VOC emissions can cause vision problems, respiratory disease, and even death [162]. Therefore, tracking VOC gas data in the atmosphere plays an essential role in ensuring the safety of persons engaged in certain activities.

Furthermore, low-dimensional carbon nanostructures like CNT, graphene, and MXene have an enormous specific surface area, making them excellent sensors for volatile organic compounds (VOCs). Therefore, nano-carbon materials, such as graphene, MXene, and CNTs, are becoming more prominent in VOC gas sensor technologies [163–165]. Wang et al. [166] effectively fabricated mesoporous ultrathin SnO_2 nanosheets in situ modulated by graphene oxide (GO), employing graphene oxide as both a sensitizer and a template. The fabricated NMs has a structure of mesoporous 2-D nano-sheets made up of tiny nanocrystals, as per the morphological characterizations. Changing the heat treatment temperature helped alter nanocrystal grain sizes, specific surface area, and GO content in 2-D GO/SnO_2 NS. The link between heat treatment temperatures and sensing characteristics was also thoroughly investigated. The best sensing efficiency was mesoporous GO/SnO_2 NS-475, which had a response value (Ra/Rg) of 2275 toward 100 ppm HCHO at 60 °C.

Moreover, the HCHO preference of 2-D GO/SnO_2 NS was very high. To the unique sensitive properties, it is possible to ascribe structural regulation and composite sensitivity in the same system, including an adequate GO content, an ultrathin nanostructure with a unique extremely thin nanostructure, nanosized SnO_2 particles, and multiple mesopores. For the investigation of the detecting capacities of GO/SnO_2 NS-475, the optimal operating temperature was determined by testing the detection capability at temperatures ranging from 35 °C to 90 °C. Figure 11a shows the sensor's reaction concerning the operating temperature. The response value was observed to rise from 40 to 60 °C for the detection of 100 ppm HCHO and then decrease from 60 to 90 °C, with a maximum value of 2275 at 60 °C. Figure 11b shows real-time variations depending on the resistance/response of the GO/SnO_2 NS-475 sensor to 100 ppm HCHO gas at 60 °C. The reaction and recovery times for GO/SnO_2 NS-475 were 81.3 and 33.7 s, correspondingly. Ultrathin nanosheet architectures decreased the transport channel for 2-D GO/SnO_2 NS, improving the gas sensor's response/recovery. It can be observed in Figure 11c that the selectivity of HCHO for the identical amounts of alcohol, acetone, toluene, NH_3, and H_2O was 32, 105, 373 (1750), and 989 for each of these compounds. As per the comparison, these sensor nodes can tolerate exposure to liquids, some VOCs, and humidity, during regular use. HCHO solution was used to make gas mixtures containing interfering compounds such as ammonia, acetone, ethanol, toluene, and water. The objective was to detect HCHO in the atmosphere using the GO/SnO_2 NS-475 sensor selectively. Figure 11d demonstrates that GO/SnO_2 NS-475 has strong anti-interference effectiveness in a complex environment. The response to interfering vapors was substantially lower than that of pure HCHO. We also explored how well the GO/SnO_2 NS-475 held up through repeated tests in 10 ppm HCHO vapor and fresh air. The sensor's reproducibility and durability were tested under these conditions. It is shown in Figure 11e that the sensitivity remained constant in intensity over all five cycles and that the curve was capable of completely returning to its pristine level, demonstrating repeatability and high stability. Figure 11f shows that after a month of evaluation, the sensor response value declined from 2270 to 1975, as shown by the arrow. Notably, the output reduction occurred primarily in the project's first week. In order to determine the thermostability of the sensor, Raman spectra were acquired before and after operation at 60 °C for a week.

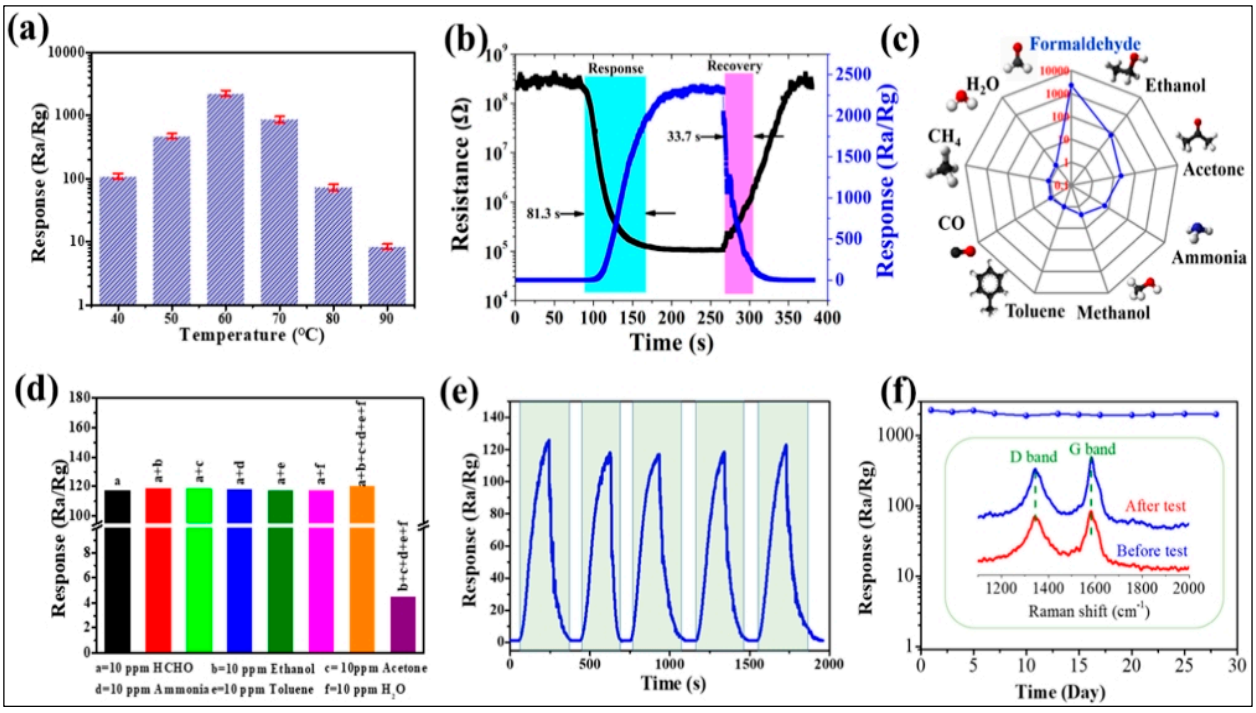

Figure 11. (**a**) Sensor responses of GO/SnO_2 nano-sheets toward 100 ppm HCHO (**b**) response/recovery graphs of the responses of the sensor based on GO/SnO_2 (**c**) polar graphs of responses of GO/SnO_2 nano-sheets sensor toward different gases (**d**) responses of the GO/SnO_2 nano-sheets sensor toward mixture (**e**) reproducibility of GO/SnO_2 nano-sheets toward mixed gases (**f**) stability of the sensor based on the responses of GO/SnO_2 nano-sheets toward 100 ppm HCHO at 60°C, the inset shows the Raman spectra of GO/SnO_2 nano-sheets. (Reprinted [166] copyright 2019 American Chemical Society).

HCHO gas may be detected using SnO_2@rGO NCs made by Rong et al. [167]. As a result of the inclusion of the rGO, these SnO_2@rGO NCs had an increased sensing response of 40 to 100 ppm for HCHO with an improved reaction time of less than one second (even less than 10 s). Additionally, the development of rGO/SnO_2 heterostructures was credited with enhancing sensing performance. As a consequence of the electron and hole migration caused by the different work functions of SnO_2 and rGO, a heterojunction of rGO@SnO_2 is formed, as illustrated in Figure 12. The presence of the rGO@SnO_2 heterojunction regulated the electronic transport characteristics of SnO_2. The thickness of the electron depletion layer on the surface of the SnO_2 material was increased due to a reduction in the number of electrons in the material. Consequently, the resistance variability and sensing sensitivity were enhanced when HCHO was applied to the sensor. An explanation of the composite's gas sensing process was also provided based on a working assumption based on the heterojunction.

MXene, like graphene structures, belongs to the 2-D materials category, which includes the newly found members of the 2-D layered materials consisting of transition metal carbides/nitrides [168]. Ti_3C_2Tx, transition metal carbide, was the first MXene material identified by etching away the Al atom from the Ti_3AlC_2 MAX phase, and it was also one of the most studied MXene materials. Such a methodology endows the Ti_3C_2Tx MXene with several functional groups, such as fluorine, oxygen, and hydroxyl groups, which improves Ti_3C_2TxMXene's adsorption characteristics toward target VOCs gases and allows it to be readily tuned as a gas sensor for VOCs detection [169–171]. The ability of the Ti_3C_2Tx-based VOCs sensor to respond to VOC analyses at room temperature has been reported. For instance, in situ XRD measurements were used by Koh et al. [172] to evaluate the interlayer spacing change of Ti_3C_2Tx MXene upon gas introduction. To investigate the relationship between film swelling behaviour and gas sensor response, N_2

and target gases/vapours employed in gas sensing tests were successively introduced to Ti_3C_2Tx MXene films inside an XRD chamber. During the measurements, Ti_3C_2Tx MXene sheets expanded preferentially when ethanol vapour was added but not when CO_2 was injected. According to the findings, the concentration of intercalated sodium ions is crucial in regulating the degree of swelling when ethanol vapour is introduced.

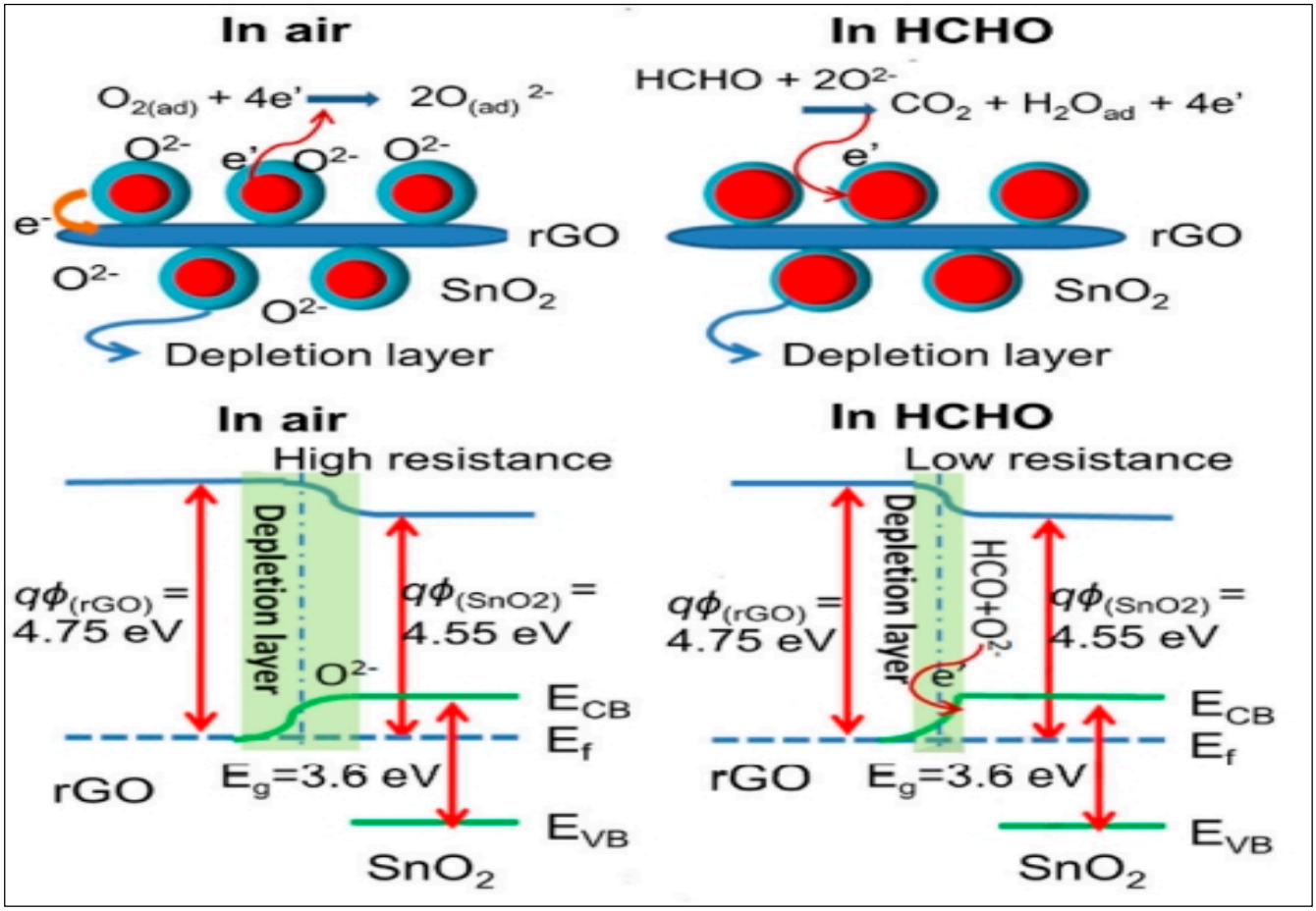

Figure 12. Graphical representation for sensing mechanism of rGO/SnO_2 sensor towards HCHO (Reprinted with permission from [167] Elsevier, License No. 5400000843096).

Furthermore, the degree of swelling corresponded to the strength of the gas reaction, with Ti_3C_2Tx MXene films treated with 0.3 mM NaOH exhibiting the greatest degree of swelling and the greatest sensitivity to ethanol. As a result, it is critical to think about pre-intercalation to improve gas sensing performance in the future. This research contributes to our understanding of MXenes' gas sensing mechanism and sheds light on how gas or vapour molecules interact with MXenes, which is crucial for sorbents, separation membranes, and other applications. Stanciu et al. [173] recently fabricated the Ti_3C_2Tx/WSe_2 hybrid using a simple surface-treating and exfoliation-based method, as illustrated in Figure 13a. Furthermore, the Ti_3C_2Tx/WSe_2 hybrid was coated on the polyimide (PI) substrate with Au interdigital electrodes using an inkjet printing method and acted as the sensing materials. Finally, by implementing a wireless monitoring system, as represented in Figure 13b, a wirelessly operating VOCs gas sensor was developed. The results showed that the Ti_3C_2Tx/WSe_2 hybrid sensor has a low LOD, reduced noise level, high accuracy, and rapid response/recovery times, paving the way for the formation of high-efficiency VOCs sensors for the next era of IoT. Another study [174] demonstrated sub-ppm VOC gas detection by simply increasing the sulfonation degree of poly(ether ether ketone)(PEEK) to 85% and mixing two types of carbon nano-fillers, CNT and fullerenes (as depicted in Figure 13c. Furthermore, the sulfonation degree of PEEK was discovered for the first

time to be favorable to methanol gas selectivity, which was a promising strategy in the development of high selectivity CH_3OH sensing devices and systems.

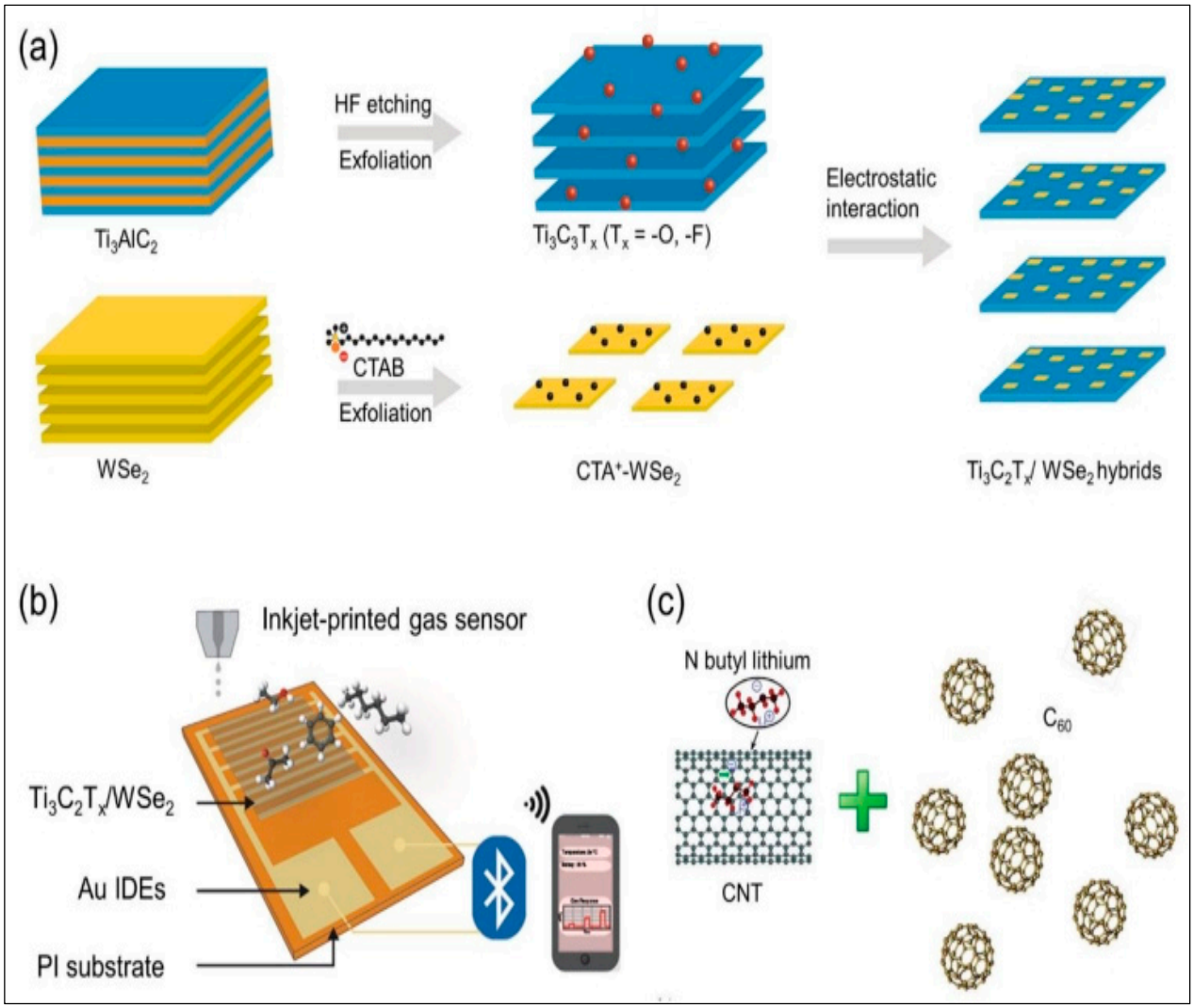

Figure 13. (**a**) Schematic representation of the Ti_3C_2Tx/WSe_2 nanohybrids fabrication. (**b**) schematic illustration of the Ti_3C_2Tx/WSe_2 sensor printed inkjet and the wireless monitoring system for VOC gas detection, (Reprinted from [173] Copyright 2020, Springer Nature, Open Access) (**c**) Representation of two types of carbon nano-fillers of CNT and fullerenes. (Reprinted [174] Copyright 2016, The Royal Society of Chemistry).

4.4. Other Environmental Applications

As a result of the introduction of nanotechnology, a whole new universe of opportunities for developing a wide range of NMs with unique capabilities for the treatment of pollutants has widened. Nanostructures are used extensively in environmental remediation activities, such as the treatment of water, air, commercial and residential wastewater, soil, and sediments. There have been diverse efficient, ecologically benign, and economically viable nano-sized materials developed via nanotechnology, each with its unique features and the ability to detoxify commercial sewage and aquatic bodies [175]. Nano-sized materials are classified as nano adsorbents, nano-catalysts, and nano-membranes based on their properties. It has been demonstrated that nano-adsorbent materials may effectively remove contaminants from wastewater and the air. Biochar, carbon nanotubes, carbon nanofibers, graphene, metals and their oxides, silica, and clay have all been applied as adsorbent materials, as have CNTs, carbon nanotube fibres, and graphene [176–178]. Researchers

have been paying close attention to NMs, such as metal oxides and semiconductors, in developing novel water treatment solutions. To break down of contaminants in wastewater, many types of nano-catalysts are utilized, and some catalysts also have antibacterial characteristics. As a result, they can also be used to remove biological pollutants [179]. In several therapeutic procedures, nano-membranes are employed. Pressure-driven wastewater treatment is an excellent method for removing pollutants from water. As a result of their small pore size, affordability, high efficiency, and environmental-friendliness, nano-membranes are commonly used to treat wastewater. When it comes to creating nano-membranes, metal NPs, non-metallic particles, and carbon-based NMs are all extensively employed [180]. It is also possible to enhance the surface characteristics of NMs by grafting functional groups onto their surfaces. This may be accomplished using a plasma technique, chemical modification, or a microwave treatment [181]. The plasma process is the most energy-efficient and ecologically friendly of the options since it requires less energy and is less harmful to the environment. Carbon-based NMs, which have been treated with metals or metal oxides, may also be capable of depleting toxic heavy metal ions [182]. According to experts, carbon-based materials will play an essential role in developing advanced energy storage systems in the near future. In addition to their extremely large surface area, mechanical capabilities, pore size distribution, and electrical characteristics, these materials are used in diverse research projects and are considered some of the most promising materials currently available. Materials, including carbon nanotubes, fullerenes, graphene, and carbon dots, are used in energy storage. Solar cells, commonly known as photovoltaic cells, were conceived by Regan and Graetzel in 1991 as a low-cost means of harvesting energy from the sun. They are now used worldwide. Photons of a given wavelength can be easily converted to energy by solar cells [183]. Thin films and crystalline silicon solar cells are the two available crystal silicon solar cells. Semiconductors such as crystalline silicon, III–V groups, cadmium telluride, and copper indium selenide/sulphide are the most popular materials utilized to produce first- and second-generation solar cells. Those economically practical devices with an easy synthesis and manufacturing procedure are included in the thin-film category [184]. Several semiconductor electrodes with a wide band gap are made possible by applying dye molecules. Among the materials used in dye-sensitized solar cells (DSSCs), platinum is the most frequent. DSSC counter electrodes are made of platinum. However, scientists are exploring alternatives due to their excessive cost and scarcity. DSSCs made of carbon-based materials have distinct characteristics, such as high conductivity, high electrochemical performance, and cheap cost, making them interesting alternatives to expensive platinum in DSSCs. All carbon-based materials, including graphene-based materials, have been applied as a medium to expedite electron transmission and maximize the dependability of photovoltaics [185–188]. The facilitating function (electron transport) of graphene-based materials is also utilized in other fields, such as batteries and fuel cells, to enhance their performance. Electrochemical energy storage devices, also known as supercapacitors, are promising next-generation energy storage devices for diverse uses, including hybrid vehicles, plug-in hybrids, portable electronic devices, and backup power cells [189–193]. This is due to multifarious features, including their high power density, excellent high stability, and very short charging time. However, even though carbon-based supercapacitors have several merits over metal-based supercapacitors, such as high energy density and cyclability, their low energy density prevents them from being used in batteries. When it comes to supercapacitors, 2-D carbon-based materials outperform 0-D and 1-D nanostructures in terms of performance. Graphene is one of the most well-known 2-D materials structures, and it is also one of the most studied. A higher level of interest in graphene than in other carbon compounds has been generated due to its high electrical conductivity, huge surface area, and big surface-to-volume ratio for applications in supercapacitors [194]. However, when utilized as electrode materials, graphene sheets have significant limitations due to their penchant for restacking, making them unsuitable for many applications. Due to the exposed surface of CNTs, which has the potential to be functionalized, and their high mechanical strength and electrical features, they are excellent candidates for energy

storage [195]. Lithium-ion batteries are another kind of energy storage material, which stores energy in the form of chemical energy and maybe recharged several times. Li-ion batteries beat capacitors in terms of energy and power density, and they have the potential to mitigate greenhouse gas emissions by a significant amount. Because of their exceptional energy efficiency, they are applied in a wide range of electrical applications. Lithium-ion batteries have lately received great interest for their potential use in both research and industry [196]. Carbon materials are often considered to be the most suitable for Li-ion batteries. They are capable of being lithiated to some degree. In addition to determining the amount of lithium that is reversibly integrated into the carbon lattice, the faradic losses experienced during the initial charge–discharge cycle and the voltage profile experienced during charging and discharging are all determined by the structure of the carbon material. Carbon-based Li-ion batteries are predicted to surpass other metal-based technologies in energy density per unit area [197,198]. This could be because they have much more energy per unit area than other metal-based technologies.

In addition to having features such as low expense, compact size, flexible porosity, easy process ability, chemical modification simplicity, carbon-based NMs such as activated carbons, 1-D carbon nanotubes, and 2-D graphene nanosheets are promising candidates for technological applications in a variety of sustainable energy storage devices. In general, increasing the specific surface area of the carbon structure and the size distribution of the pores allows for increased electrochemical capacitance efficiency in terms of both power delivery rate and energy storage capacity, as seen in the figure below. Table 1 depicts a variety of published publications illustrating diverse carbon NMs created from green synthesis (plant extracts) that have been used for diverse environmental uses, as shown in the articles.

Table 1. Various carbon NMs employed for diverse environmental applications.

Analyte	Nanoparticles Extracted	Method	Application	References
Camphor Oil	Multiwall Carbon nanotube	CVD precursor	Photocatalytic	[199]
Chicken Eggs	Carbon Dots	Plasma Induced	Silk-screen printing, Inkjet	[141]
Neem Oil	Multiwall Carbon nanotube	Pyrolysis	Graphitization, Catalytic	[200]
Hibiscus tiliaceus	MWCNTs	Raman spectroscopy	Gas sensing or water remediation	[201]
Terminalia chebula	Graphene nanosheets	UV–Vis analysis	Nanoelectronics, Composites, fuel cells, supercapacitor, sensors and catalysis	[202]
Eucalyptus	rGO	Adsorption	Bioreduction	[99]
Rice Hull	Carbon Dots	Hydrothermal	Alcohol vapor detection	[203]
Chickpea	Fluorescent CNTs	Pyrolysis	Bioimaging	[204]
Larch	Carbon nanodots	Hydrothermal	Photocatalysis	[205]
Au@CQD	CQDs	-	Photocatalyst, H_2 Production	[206]
CNNS@CQDs	Carbon Nanosheets and Quantum dots	-	Photocatalyst, H_2 Production	[207]
Wheat husk	Carbon dots	Hydrothermal	Cellular Imaging, F^- ion detection	[208]
Pineapple rind	CQD	Hydrothermal	determination of Hg_{2+}, electronic security devices	[209]
Durian skin	Carbon dots	Pyrolysis	Supercapacitor Electrode	[210]
Apple rind	Carbon dots	charring	photodegradation	[211]
Tea leaf waste	CQD	Oxidative pyrolysis	Gefitinib sensor	[109]
CdS/BCN	Carbon NPs	-	CO_2 Reduction, Photocatalyst	[212]
SiNW@CQDs	Carbon Quantum Nanodots	-	Optoelectronic Devices	[213]
Bi-NRs@NCNTs	Caarbon Nanotubes	-	CO_2 Reduction, electrocatalyst	[214]
$RuTiO_2$	MWCNTs	-	CPE (Chlorinated Polyethylene) Liquid Level Sensors	[215]
SWCNTs@Gold NPs	Carbon Nanotubes	-	Gas sensing	[216]
MO_2C@CNT	Carbon Nanotubes	-	Hydrogen Generation	[217]
C@NiO	Carbon Dots	Calcination	Supercapacitor	[218]
Mn_3O_4@CNP	Carbon NPs	-	Supercapacitor	[219]
B@CNPs	Carbon NPs	Hydrothermal	Bioimaging	[220]

5. Conclusions and Future Prospectus

There is an urgent need for organic compounds and heavy hydrocarbons to address the growing demand for carbon-based nanostructures in emerging areas, including sensors, biomedicine, supercapacitors, and gas storage. In order to safeguard the environment and human health, wastewater treatment, especially industrial wastewater, is critical and required. Environmental pollution prevention has made considerable strides in recent years, as seen by this summary. Some sophisticated technologies that can be utilized for wastewater treatment include greener nanotechnology and sustainable NPs that can be used to remediate dangerous pollutants. Carbon-based NPs may have an advantage over other types of NPs in terms of infrastructure and resource use, as well as concerns regarding the dangerous qualities of NPs. Using CNTs, CQDs, GQDs, and graphene-based NPs to clean up the environment and save resources may be better than traditional treatment NMs. Despite the significant advancements in synthesis and the catalytic capabilities shown by green NPs, such as CNTs, CQDs, GQDs, and graphene-based NPs, future research should pay greater attention to the following issues:

- Innovative and revolutionary synthetic approaches are required to minimize the cost of NM synthesis and enhancing their catalytic performance.
- Bio-waste-derived NPs have been used to remediate wastewater.
- Magnetic NPs for water purification have been improved and reused.
- Deception of animal residues, such as bone, bristles, and eggshells, for NM fabrication.
- Natural minerals, such as bentonite, clays, zeolites, and montmorillonite, are being used as non-noxious, low-cost, and plentiful substrates for the biosynthesis of NPs and their environmental applications.
- For all of the aforementioned ideas, toxicity studies should be completed. Full analyses of NMs hazards and possible effects on human health and ecosystems, including potential cellular toxicities, should be investigated and evaluated.

Author Contributions: Conceptualization, V.D. and R.V.; resources, K.M.B. and R.J.; writing—original draft preparation, V.D. and S.G.; writing—review and editing, C.G., R.B. and S.G.; supervision, A.C. and K.-Y.A.L.; funding acquisition, M.-H.Y. All authors have read and agreed to the published version of the manuscript.

Funding: This study was financially supported in part by the Ministry of Science and Technology, Taipei, Taiwan (MOST 111-2221-E-039-005) and China Medical University, Taichung, Taiwan (CMU110-MF-36).

Institutional Review Board Statement: Not applicable.

Informed Consent Statement: Not applicable.

Data Availability Statement: Not applicable.

Acknowledgments: Author V.D. is thankful to the Vice-chancellor of Shoolini University for his constant motivation.

Conflicts of Interest: The authors declare no conflict of interest.

References

1. Kavitha, S.; Umadevi, M.; Janani, S.; Balakrishnan, T.; Ramanibai, R. Fluorescence quenching and photocatalytic degradation of textile dyeing waste water by silver nanoparticles. *Spectrochim. Acta Part A Mol. Biomol. Spectrosc.* **2014**, *127*, 115–121. [CrossRef] [PubMed]
2. Rajabi, H.R.; Arjmand, H.; Hoseini, S.J.; Nasrabadi, H. Surface modified magnetic nanoparticles as efficient and green sorbents: Synthesis, characterization, and application for the removal of anionic dye. *J. Magn. Magn. Mater.* **2015**, *394*, 7–13. [CrossRef]
3. Ranjithkumar, V.; Sangeetha, S.; Vairam, S. Synthesis of magnetic activated carbon/α-Fe_2O_3 nanocomposite and its application in the removal of acid yellow 17 dye from water. *J. Hazard. Mater.* **2014**, *273*, 127–135. [CrossRef] [PubMed]
4. Nassar, N.N.; Marei, N.N.; Vitale, G.; Arar, L.A. Adsorptive removal of dyes from synthetic and real textile wastewater using magnetic iron oxide nanoparticles: Thermodynamic and mechanistic insights. *Can. J. Chem. Eng.* **2015**, *93*, 1965–1974. [CrossRef]

5. Dutta, V.; Singh, P.; Shandilya, P.; Sharma, S.; Raizada, P.; Saini, A.K.; Gupta, V.K.; Hosseini-Bandegharaei, A.; Agarwal, S.; Rahmani-Sani, A. Review on advances in photocatalytic water disinfection utilizing graphene and graphene derivatives-based nanocomposites. *J. Environ. Chem. Eng.* **2019**, *7*, 103132. [CrossRef]
6. Garole, V.; Choudhary, B.; Tetgure, S.; Garole, D.; Borse, A. Detoxification of toxic dyes using biosynthesized iron nanoparticles by photo-Fenton processes. *Int. J. Environ. Sci. Technol.* **2018**, *15*, 1649–1656. [CrossRef]
7. Abdellatif, H.R.; Zhang, G.; Wang, X.; Xie, D.; Irvine, J.T.; Ni, J.; Ni, C. Boosting photocatalytic oxidation on graphitic carbon nitride for efficient photocatalysis by heterojunction with graphitic carbon units. *Chem. Eng. J.* **2019**, *370*, 875–884. [CrossRef]
8. Akhavan, O.; Ghaderi, E.; Esfandiar, A. Wrapping bacteria by graphene nanosheets for isolation from environment, reactivation by sonication, and inactivation by near-infrared irradiation. *J. Phys. Chem. B* **2011**, *115*, 6279–6288. [CrossRef]
9. Kumar, A.; Hasija, V.; Sudhaik, A.; Raizada, P.; Van Le, Q.; Singh, P.; Pham, T.-H.; Kim, T.; Ghotekar, S.; Nguyen, V.-H. Artificial leaf for light-driven CO_2 reduction: Basic concepts, advanced structures and selective solar-to-chemical products. *Chem. Eng. J.* **2022**, *430*, 133031. [CrossRef]
10. Ali, M.M.; Nair, J.A.; Sandhya, K. Role of reactive oxygen species in the visible light photocatalytic mineralization of rhodamine B dye by P25–carbon dot photocatalyst. *Dye. Pigment.* **2019**, *163*, 274–284.
11. Ali, Q.; Ahmed, W.; Lal, S.; Sen, T. Novel multifunctional carbon nanotube containing silver and iron oxide nanoparticles for antimicrobial applications in water treatment. *Mater. Today Proc.* **2017**, *4*, 57–64. [CrossRef]
12. Ghotekar, S.; Pansambal, S.; Lin, K.-Y.A.; Pore, D.; Oza, R. Recent Advances in Synthesis of $CeVO_4$ Nanoparticles and Their Potential Scaffold for Photocatalytic Applications. *Top. Catal.* **2022**, 1–15. [CrossRef]
13. Kumar, R.; Raizada, P.; Khan, A.A.P.; Nguyen, V.-H.; Van Le, Q.; Ghotekar, S.; Selvasembian, R.; Gandhi, V.; Singh, A.; Singh, P. Recent progress in emerging $BiPO_4$-based photocatalysts: Synthesis, properties, modification strategies, and photocatalytic applications. *J. Mater. Sci. Technol.* **2022**, *108*, 208–225. [CrossRef]
14. An, X.; Li, K.; Tang, J. Cu_2O/reduced graphene oxide composites for the photocatalytic conversion of CO_2. *ChemSusChem* **2014**, *7*, 1086–1093. [CrossRef] [PubMed]
15. Cuong, H.N.; Pansambal, S.; Ghotekar, S.; Oza, R.; Hai, N.T.T.; Viet, N.M.; Nguyen, V.-H. New frontiers in the plant extract mediated biosynthesis of copper oxide (CuO) nanoparticles and their potential applications: A review. *Environ. Res.* **2022**, *203*, 111858. [CrossRef] [PubMed]
16. Kashid, Y.; Ghotekar, S.; Bilal, M.; Pansambal, S.; Oza, R.; Varma, R.S.; Nguyen, V.-H.; Murthy, H.A.; Mane, D. Bio-inspired sustainable synthesis of silver chloride nanoparticles and their prominent applications. *J. Indian Chem. Soc.* **2022**, *99*, 100335. [CrossRef]
17. Ani, I.; Akpan, U.; Olutoye, M.; Hameed, B. Photocatalytic degradation of pollutants in petroleum refinery wastewater by TiO_2-and ZnO-based photocatalysts: Recent development. *J. Clean. Prod.* **2018**, *205*, 930–954. [CrossRef]
18. Antoniadou, M.; Daskalaki, V.M.; Balis, N.; Kondarides, D.I.; Kordulis, C.; Lianos, P. Photocatalysis and photoelectrocatalysis using (CdS-ZnS)/TiO_2 combined photocatalysts. *Appl. Catal. B Environ.* **2011**, *107*, 188–196. [CrossRef]
19. Baek, S.; Joo, S.H.; Su, C.; Toborek, M. Antibacterial effects of graphene-and carbon-nanotube-based nanohybrids on Escherichia coli: Implications for treating multidrug-resistant bacteria. *J. Environ. Manag.* **2019**, *247*, 214–223. [CrossRef]
20. Bajorowicz, B.; Kobylański, M.P.; Gołąbiewska, A.; Nadolna, J.; Zaleska-Medynska, A.; Malankowska, A. Quantum dot-decorated semiconductor micro-and nanoparticles: A review of their synthesis, characterization and application in photocatalysis. *Adv. Colloid Interface Sci.* **2018**, *256*, 352–372. [CrossRef]
21. Banerjee, D.; Bhowmick, P.; Pahari, D.; Santra, S.; Sarkar, S.; Das, B.; Chattopadhyay, K. Pseudo first ordered adsorption of noxious textile dyes by low-temperature synthesized amorphous carbon nanotubes. *Phys. E Low-Dimens. Syst. Nanostructures* **2017**, *87*, 68–76. [CrossRef]
22. Barati, A.; Shamsipur, M.; Arkan, E.; Hosseinzadeh, L.; Abdollahi, H. Synthesis of biocompatible and highly photoluminescent nitrogen doped carbon dots from lime: Analytical applications and optimization using response surface methodology. *Mater. Sci. Eng. C* **2015**, *47*, 325–332. [CrossRef] [PubMed]
23. Bohdziewicz, J.; Kamińska, G. Kinetics and equilibrium of the sorption of bisphenol A by carbon nanotubes from wastewater. *Water Sci. Technol.* **2013**, *68*, 1306–1314. [CrossRef] [PubMed]
24. Dabhane, H.; Ghotekar, S.; Tambade, P.; Pansambal, S.; Oza, R.; Medhane, V. MgO nanoparticles: Synthesis, characterization, and applications as a catalyst for organic transformations. *Eur. J. Chem.* **2021**, *12*, 86–108. [CrossRef]
25. Cai, W.; Chen, X. Nanoplatforms for targeted molecular imaging in living subjects. *Small* **2007**, *3*, 1840–1854. [CrossRef] [PubMed]
26. Cha, S.I.; Kim, K.T.; Lee, K.H.; Mo, C.B.; Jeong, Y.J.; Hong, S.H. Mechanical and electrical properties of cross-linked carbon nanotubes. *Carbon* **2008**, *46*, 482–488. [CrossRef]
27. Chai, Y.-Y.; Qu, D.-P.; Ma, D.-K.; Chen, W.; Huang, S. Carbon quantum dots/Zn^{2+} ions doped-CdS nanowires with enhanced photocatalytic activity for reduction of 4-nitroaniline to p-phenylenediamine. *Appl. Surf. Sci.* **2018**, *450*, 1–8. [CrossRef]
28. Chan, W.C.; Maxwell, D.J.; Gao, X.; Bailey, R.E.; Han, M.; Nie, S. Luminescent quantum dots for multiplexed biological detection and imaging. *Curr. Opin. Biotechnol.* **2002**, *13*, 40–46. [CrossRef]
29. Kelele, K.G.; Tadesse, A.; Desalegn, T.; Ghotekar, S.; Balachandran, R.; Murthy, H.C.A. Synthesis and characterizations of metal ions doped barium strontium titanate (BST) nanomaterials for photocatalytic and electrical applications: A mini review. *Int. J. Mater. Res.* **2021**, *112*, 665–677. [CrossRef]

30. Das, R.; Ali, M.E.; Abd Hamid, S.B.; Ramakrishna, S.; Chowdhury, Z.Z. Carbon nanotube membranes for water purification: A bright future in water desalination. *Desalination* **2014**, *336*, 97–109. [CrossRef]
31. Kalra, A.; Gupta, A. Recent advances in decolourization of dyes using iron nanoparticles: A mini review. *Mater. Today Proc.* **2021**, *36*, 689–696. [CrossRef]
32. Ghotekar, S.; Pansambal, S.; Bilal, M.; Pingale, S.S.; Oza, R. Environmentally friendly synthesis of Cr_2O_3 nanoparticles: Characterization, applications and future perspective—A review. *Case Stud. Chem. Environ. Eng.* **2021**, *3*, 100089. [CrossRef]
33. Ghotekar, S.; Pagar, K.; Pansambal, S.; Murthy, H.; Oza, R. A review on eco-friendly synthesis of $BiVO_4$ nanoparticle and its eclectic applications. *Adv. J. Sci. Eng.* **2020**, *30*, 106–112.
34. Korde, P.; Ghotekar, S.; Pagar, T.; Pansambal, S.; Oza, R.; Mane, D. Plant extract assisted eco-benevolent synthesis of selenium nanoparticles-a review on plant parts involved, characterization and their recent applications. *J. Chem. Rev.* **2020**, *2*, 157–168.
35. Ghotekar, S. A review on plant extract mediated biogenic synthesis of CdO nanoparticles and their recent applications. *Asian J. Green Chem.* **2019**, *3*, 187–200.
36. Nikam, A.; Pagar, T.; Ghotekar, S.; Pagar, K.; Pansambal, S. A review on plant extract mediated green synthesis of zirconia nanoparticles and their miscellaneous applications. *J. Chem. Rev.* **2019**, *1*, 154–163.
37. Dalvand, A.; Nabizadeh, R.; Ganjali, M.R.; Khoobi, M.; Nazmara, S.; Mahvi, A.H. Modeling of Reactive Blue 19 azo dye removal from colored textile wastewater using L-arginine-functionalized Fe_3O_4 nanoparticles: Optimization, reusability, kinetic and equilibrium studies. *J. Magn. Magn. Mater.* **2016**, *404*, 179–189. [CrossRef]
38. Yang, J.; Tian, Z.; Yin, C.; Cui, W.; Qian, Wei, F. Carbon nanotube-and graphene-based nanomaterials and applications in high-voltage supercapacitor: A review. *Carbon* **2019**, *141*, 467–480. [CrossRef]
39. Murthy, H.; Ghotekar, S.; Vinay Kumar, B.; Roy, A. Graphene: A Multifunctional Nanomaterial with Versatile Applications. *Adv. Mater. Sci. Eng.* **2021**, *2021*, 2418149. [CrossRef]
40. Dutta, V.; Devasia, J.; Chauhan, A.; Jayalakshmi, M.; Vasantha, V.; Jha, A.; Nizam, A.; Lin, K.-Y.A.; Ghotekar, S. Photocatalytic nanomaterials: Applications for remediation of toxic polycyclic aromatic hydrocarbons and green management. *Chem. Eng. J. Adv.* **2022**, *11*, 100353. [CrossRef]
41. Ji, H.; Sellan, D.P.; Pettes, M.T.; Kong, X.; Ji, J.; Shi, L.; Ruoff, R.S. Enhanced thermal conductivity of phase change materials with ultrathin-graphite foams for thermal energy storage. *Energy Environ. Sci.* **2014**, *7*, 1185–1192. [CrossRef]
42. Canseco, V.; Anguy, Y.; Roa, J.J.; Palomo, E. Structural and mechanical characterization of graphite foam/phase change material composites. *Carbon* **2014**, *74*, 266–281. [CrossRef]
43. Zhong, Y.; Li, S.; Wei, X.; Liu, Z.; Guo, Q.; Shi, J.; Liu, L. Heat transfer enhancement of paraffin wax using compressed expanded natural graphite for thermal energy storage. *Carbon* **2010**, *48*, 300–304. [CrossRef]
44. Lafdi, K.; Mesalhy, O.; Elgafy, A. Graphite foams infiltrated with phase change materials as alternative materials for space and terrestrial thermal energy storage applications. *Carbon* **2008**, *46*, 159–168. [CrossRef]
45. Mesalhy, O.; Lafdi, K.; Elgafy, A. Carbon foam matrices saturated with PCM for thermal protection purposes. *Carbon* **2006**, *44*, 2080–2088. [CrossRef]
46. Kholmanov, I.; Kim, J.; Ou, E.; Ruoff, R.S.; Shi, L. Continuous carbon nanotube–ultrathin graphite hybrid foams for increased thermal conductivity and suppressed subcooling in composite phase change materials. *ACS Nano* **2015**, *9*, 11699–11707. [CrossRef]
47. Kockrick, E.; Schrage, C.; Borchardt, L.; Klein, N.; Rose, M.; Senkovska, I.; Kaskel, S. Ordered mesoporous carbide derived carbons for high pressure gas storage. *Carbon* **2010**, *48*, 1707–1717. [CrossRef]
48. Liu, J.; Zhou, Y.; Sun, Y.; Su, W.; Zhou, L. Methane storage in wet carbon of tailored pore sizes. *Carbon* **2011**, *49*, 3731–3736. [CrossRef]
49. Thostenson, E.T.; Chou, T.-W. Processing-structure-multi-functional property relationship in carbon nanotube/epoxy composites. *Carbon* **2006**, *44*, 3022–3029. [CrossRef]
50. Sharma, S.; Dutta, V.; Singh, P.; Raizada, P.; Rahmani-Sani, A.; Hosseini-Bandegharaei, A.; Thakur, V.K. Carbon quantum dot supported semiconductor photocatalysts for efficient degradation of organic pollutants in water: A review. *J. Clean. Prod.* **2019**, *228*, 755–769. [CrossRef]
51. Wu, H.C.; Huy, N.N.; Kwon, E.; Lin, J.-Y.; Jaree, A.; Lee, J.; Ghotekar, S.; Duan, X.; Tuan, D.D.; Lin, K.-Y.A. Metal-free and oxidizing agent-free ultra-selective catalytic aerobic conversion of vanillyl alcohol to vanillin by carbon fiber. *J. Taiwan Inst. Chem. Eng.* **2022**, 104492. [CrossRef]
52. Li, D.; Zhou, J.; Zhang, Z.; Li, L.; Tian, Y.; Lu, Y.; Qiao, J.; Li, L.; Wen, L. Improving low-pressure CO_2 capture performance of N-doped active carbons by adjusting flow rate of protective gas during alkali activation. *Carbon* **2017**, *114*, 496–503. [CrossRef]
53. Mao, P.-H.; Huy, N.N.; Ghotekar, S.; Lin, J.-Y.; Kwon, E.; Yeoh, F.-Y.; Ghanbari, F.; Lisak, G.; Lin, K.-Y.A. Single-Step Synthesized Functionalized Copper Carboxylate Framework Meshes as Hierarchical Catalysts for Enhanced Reduction of Nitrogen-Containing Phenolic Contaminants. *Catalysts* **2022**, *12*, 765. [CrossRef]
54. Kante, K.; Florent, M.; Temirgaliyeva, A.; Lesbayev, B.; Bandosz, T.J. Exploring resistance changes of porous carbon upon physical adsorption of VOCs. *Carbon* **2019**, *146*, 568–571. [CrossRef]
55. Blanco, F.; Vilanova, X.; Fierro, V.; Celzard, A.; Ivanov, P.; Llobet, E.; Cañellas, N.; Ramírez, J.; Correig, X. Fabrication and characterisation of microporous activated carbon-based pre-concentrators for benzene vapours. *Sens. Actuators B Chem.* **2008**, *132*, 90–98. [CrossRef]

56. Van Thuan, D.; Nguyen, T.L.; Thi, H.H.P.; Thanh, N.T.; Ghotekar, S.; Sharma, A.K.; Binh, M.T.; Nga, T.T.; Pham, T.-D.; Cam, D.P. Development of Indium vanadate and Silver deposited on graphitic carbon nitride ternary heterojunction for advanced photocatalytic degradation of residual antibiotics in aqueous environment. *Opt. Mater.* **2022**, *123*, 111885. [CrossRef]
57. Travlou, N.A.; Bandosz, T.J. N-doped polymeric resin-derived porous carbons as efficient ammonia removal and detection media. *Carbon* **2017**, *117*, 228–239. [CrossRef]
58. Jiang, D.-E.; Cooper, V.R.; Dai, S. Porous graphene as the ultimate membrane for gas separation. *Nano Lett.* **2009**, *9*, 4019–4024. [CrossRef] [PubMed]
59. Seredych, M.; Hulicova-Jurcakova, D.; Lu, G.Q.; Bandosz, T.J. Surface functional groups of carbons and the effects of their chemical character, density and accessibility to ions on electrochemical performance. *Carbon* **2008**, *46*, 1475–1488. [CrossRef]
60. Hola, K.; Bourlinos, A.B.; Kozak, O.; Berka, K.; Siskova, K.M.; Havrdova, M.; Tucek, J.; Safarova, K.; Otyepka, M.; Giannelis, E.P. Photoluminescence effects of graphitic core size and surface functional groups in carbon dots: COO− induced red-shift emission. *Carbon* **2014**, *70*, 279–286. [CrossRef]
61. Hu, J.; Shao, D.; Chen, C.; Sheng, G.; Ren, X.; Wang, X. Removal of 1-naphthylamine from aqueous solution by multiwall carbon nanotubes/iron oxides/cyclodextrin composite. *J. Hazard. Mater.* **2011**, *185*, 463–471. [CrossRef]
62. Hu, L.; Sun, Y.; Li, S.; Wang, X.; Hu, K.; Wang, L.; Liang, X.-j.; Wu, Y. Multifunctional carbon dots with high quantum yield for imaging and gene delivery. *Carbon* **2014**, *67*, 508–513. [CrossRef]
63. Huang, Z.-H.; Zheng, X.; Lv, W.; Wang, M.; Yang, Q.-H.; Kang, F. Adsorption of lead (II) ions from aqueous solution on low-temperature exfoliated graphene nanosheets. *Langmuir* **2011**, *27*, 7558–7562. [CrossRef]
64. Jackson, P.; Jacobsen, N.R.; Baun, A.; Birkedal, R.; Kühnel, D.; Jensen, K.A.; Vogel, U.; Wallin, H. Bioaccumulation and ecotoxicity of carbon nanotubes. *Chem. Cent. J.* **2013**, *7*, 154. [CrossRef]
65. Jeon, S.; Yun, J.; Lee, Y.-S.; Kim, H.-I. Removal of Cu (II) ions by Alginate/Carbon Nanotube/Maghemite Composite Magnetic Beads. *Carbon Lett.* **2010**, *11*, 117–121. [CrossRef]
66. Ji, L.; Chen, W.; Duan, L.; Zhu, D. Mechanisms for strong adsorption of tetracycline to carbon nanotubes: A comparative study using activated carbon and graphite as adsorbents. *Environ. Sci. Technol.* **2009**, *43*, 2322–2327. [CrossRef]
67. Jiang, K.; Sun, S.; Zhang, L.; Lu, Y.; Wu, A.; Cai, C.; Lin, H. Red, green, and blue luminescence by carbon dots: Full-color emission tuning and multicolor cellular imaging. *Angew. Chem. Int. Ed.* **2015**, *54*, 5360–5363. [CrossRef]
68. Jiang, L.; Fan, Z. Design of advanced porous graphene materials: From graphene nanomesh to 3D architectures. *Nanoscale* **2014**, *6*, 1922–1945. [CrossRef]
69. Jones, S.; Pramanik, A.; Kanchanapally, R.; Viraka Nellore, B.P.; Begum, S.; Sweet, C.; Ray, P.C. Multifunctional three-dimensional chitosan/gold nanoparticle/graphene oxide architecture for separation, label-free SERS identification of pharmaceutical contaminants, and effective killing of superbugs. *ACS Sustain. Chem. Eng.* **2017**, *5*, 7175–7187.
70. Julkapli, N.M.; Bagheri, S. Graphene supported heterogeneous catalysts: An overview. *Int. J. Hydrogen Energy* **2015**, *40*, 948–979. [CrossRef]
71. Kabbashi, N.A.; Atieh, M.A.; Al-Mamun, A.; Mirghami, M.E.; Alam, M.D.Z.; Yahya, N. Kinetic adsorption of application of carbon nanotubes for Pb (II) removal from aqueous solution. *J. Environ. Sci.* **2009**, *21*, 539–544. [CrossRef]
72. Kaur, M.; Kaur, M.; Sharma, V.K. Nitrogen-doped graphene and graphene quantum dots: A review onsynthesis and applications in energy, sensors and environment. *Adv. Colloid Interface Sci.* **2018**, *259*, 44–64. [CrossRef] [PubMed]
73. Kaur, S.; Sharma, S.; Kansal, S.K. Synthesis of ZnS/CQDs nanocomposite and its application as a photocatalyst for the degradation of an anionic dye, ARS. *Superlattices Microstruct.* **2016**, *98*, 86–95. [CrossRef]
74. Ke, J.; Li, X.; Zhao, Q.; Liu, B.; Liu, S.; Wang, S. Upconversion carbon quantum dots as visible light responsive component for efficient enhancement of photocatalytic performance. *J. Colloid Interface Sci.* **2017**, *496*, 425–433. [CrossRef] [PubMed]
75. Kemp, K.C.; Seema, H.; Saleh, M.; Le, N.H.; Mahesh, K.; Chandra, V.; Kim, K.S. Environmental applications using graphene composites: Water remediation and gas adsorption. *Nanoscale* **2013**, *5*, 3149–3171. [CrossRef]
76. Yan, T.; Liu, J.; Lei, H.; Shi, L.; An, Z.; Park, H.S.; Zhang, D. Capacitive deionization of saline water using sandwich-like nitrogen-doped graphene composites via a self-assembling strategy. *Environ. Sci. Nano* **2018**, *5*, 2722–2730. [CrossRef]
77. Khan, A.; Goepel, M.; Colmenares, J.C.; Gläser, R. Chitosan-based N-doped carbon materials for electrocatalytic and photocatalytic applications. *ACS Sustain. Chem. Eng.* **2020**, *8*, 4708–4727. [CrossRef]
78. Khin, M.M.; Nair, A.S.; Babu, V.J.; Murugan, R.; Ramakrishna, S. A review on nanomaterials for environmental remediation. *Energy Environ. Sci.* **2012**, *5*, 8075–8109. [CrossRef]
79. Kongkanand, A.; Kamat, P.V. Electron storage in single wall carbon nanotubes. Fermi level equilibration in semiconductor–SWCNT suspensions. *ACS Nano* **2007**, *1*, 13–21. [CrossRef]
80. Konicki, W.; Pełech, I.; Mijowska, E.; Jasińska, I. Adsorption of anionic dye Direct Red 23 onto magnetic multi-walled carbon nanotubes-Fe3C nanocomposite: Kinetics, equilibrium and thermodynamics. *Chem. Eng. J.* **2012**, *210*, 87–95. [CrossRef]
81. Xu, X.; Ray, R.; Gu, Y.; Ploehn, H.J.; Gearheart, L.; Raker, K.; Scrivens, W.A. Electrophoretic analysis and purification of fluorescent single-walled carbon nanotube fragments. *J. Am. Chem. Soc.* **2004**, *126*, 12736–12737. [CrossRef]
82. Sun, Y.-P.; Zhou, B.; Lin, Y.; Wang, W.; Fernando, K.S.; Pathak, P.; Meziani, M.J.; Harruff, B.A.; Wang, X.; Wang, H. Quantum-sized carbon dots for bright and colorful photoluminescence. *J. Am. Chem. Soc.* **2006**, *128*, 7756–7757. [CrossRef]
83. Kumar, R.; Khan, M.A.; Haq, N. Application of carbon nanotubes in heavy metals remediation. *Crit. Rev. Environ. Sci. Technol.* **2014**, *44*, 1000–1035. [CrossRef]

84. Kuo, C.-Y.; Lin, H.-Y. Adsorption of aqueous cadmium (II) onto modified multi-walled carbon nanotubes following microwave/chemical treatment. *Desalination* **2009**, *249*, 792–796. [CrossRef]
85. Lee, W.J.; Lee, J.M.; Kochuveedu, S.T.; Han, T.H.; Jeong, H.Y.; Park, M.; Yun, J.M.; Kwon, J.; No, K.; Kim, D.H. Biomineralized N-doped CNT/TiO_2 core/shell nanowires for visible light photocatalysis. *ACS Nano* **2012**, *6*, 935–943. [CrossRef]
86. Li, G.; Wang, F.; Liu, P.; Chen, Z.; Lei, P.; Xu, Z.; Li, Z.; Ding, Y.; Zhang, S.; Yang, M. Polymer dots grafted TiO_2 nanohybrids as high performance visible light photocatalysts. *Chemosphere* **2018**, *197*, 526–534. [CrossRef]
87. Li, H.; He, X.; Kang, Z.; Huang, H.; Liu, Y.; Liu, J.; Lian, S.; Tsang, C.H.A.; Yang, X.; Lee, S.T. Water-soluble fluorescent carbon quantum dots and photocatalyst design. *Angew. Chem. Int. Ed.* **2010**, *49*, 4430–4434. [CrossRef]
88. Chen, L.C.; Teng, C.Y.; Lin, C.Y.; Chang, H.Y.; Chen, S.J.; Teng, H. Architecting nitrogen functionalities on graphene oxide photocatalysts for boosting hydrogen production in water decomposition process. *Adv. Energy Mater.* **2016**, *6*, 1600719. [CrossRef]
89. Chorawalaa, K.K.; Mehta, M.J. Applications of nanotechnology in wastewater treatment. *Int. J. Innov. Emerg. Res. Eng.* **2015**, *2*, 21–26.
90. Chu, K.-W.; Lee, S.L.; Chang, C.-J.; Liu, L. Recent progress of carbon dot precursors and photocatalysis applications. *Polymers* **2019**, *11*, 689. [CrossRef] [PubMed]
91. Li, W.; Xie, S.; Qian, L.X.; Chang, B.; Zou, B.; Zhou, W.; Zhao, R.; Wang, G. Large-scale synthesis of aligned carbon nanotubes. *Science* **1996**, *274*, 1701–1703. [CrossRef]
92. Bronikowski, M.J. CVD growth of carbon nanotube bundle arrays. *Carbon* **2006**, *44*, 2822–2832. [CrossRef]
93. Mayne, M.; Grobert, N.; Terrones, M.; Kamalakaran, R.; Rühle, M.; Kroto, H.; Walton, D. Pyrolytic production of aligned carbon nanotubes from homogeneously dispersed benzene-based aerosols. *Chem. Phys. Lett.* **2001**, *338*, 101–107. [CrossRef]
94. Zhang, Z.; Wei, B.; Ramanath, G.; Ajayan,P. Substrate-site selective growth of aligned carbon nanotubes. *Appl. Phys. Lett.* **2000**, *77*, 3764–3766. [CrossRef]
95. Sen, R.; Govindaraj, A.; Rao, C. Carbon nanotubes by the metallocene route. *Chem. Phys. Lett.* **1997**, *267*, 276–280. [CrossRef]
96. Sharma, S.; Kalita, G.; Hirano, R.; Hayashi, Y.; Tanemura, M. Influence of gas composition on the formation of graphene domain synthesized from camphor. *Mater. Lett.* **2013**, *93*, 258–262. [CrossRef]
97. Afre, R.A.; Soga, T.; Jimbo, T.; Kumar, M.; Ando, Y.; Sharon, M.; Somani, P.R.; Umeno, M. Carbon nanotubes by spray pyrolysis of turpentine oil at different temperatures and their studies. *Microporous Mesoporous Mater.* **2006**, *96*, 184–190. [CrossRef]
98. Ghosh, P.; Afre, R.A.; Soga, T.; Jimbo, T. A simple method of producing single-walled carbon nanotubes from a natural precursor: Eucalyptus oil. *Mater. Lett.* **2007**, *61*, 3768–3770. [CrossRef]
99. Kumar, R.; Tiwari, R.S.; Srivastava, O.N. Scalable synthesis of aligned carbon nanotubes bundles using green natural precursor: Neem oil. *Nanoscale Res. Lett.* **2011**, *6*, 92. [CrossRef] [PubMed]
100. Terrones, M. Science and technology of the twenty-first century: Synthesis, properties, and applications of carbon nanotubes. *Annu. Rev. Mater. Res.* **2003**, *33*, 419–501. [CrossRef]
101. Ajayan, P.; Stephan, O.; Colliex, C.; Trauth, D. Aligned carbon nanotube arrays formed by cutting a polymer resin—Nanotube composite. *Science* **1994**, *265*, 1212–1214. [CrossRef] [PubMed]
102. Andrews, R.; Jacques, D.; Rao, A.; Derbyshire, F.; Qian, D.; Fan, X.; Dickey, E.; Chen, J. Continuous production of aligned carbon nanotubes: A step closer to commercial realization. *Chem. Phys. Lett.* **1999**, *303*, 467–474. [CrossRef]
103. Fan, S.; Chapline, M.G.; Franklin, N.R.; Tombler, T.W.; Cassell, A.M.; Dai, H. Self-oriented regular arrays of carbon nanotubes and their field emission properties. *Science* **1999**, *283*, 512–514. [CrossRef]
104. Wang, C.; Li, D.; Lu, Z.; Song, M.; Xia, W. Synthesis of carbon nanoparticles in a non-thermal plasma process. *Chem. Eng. Sci.* **2020**, *227*, 115921. [CrossRef]
105. Nguyen, V.; Zhao, N.; Yan, L.; Zhong, P.; Le, P.H. Double-pulse femtosecond laser ablation for synthesis of ultrasmall carbon nanodots. *Mater. Res. Express* **2020**, *7*, 015606. [CrossRef]
106. Ngu, P.Z.Z.; Chia, S.P.P.; Fong, J.F.Y.; Ng, S.M. Synthesis of carbon nanoparticles from waste rice husk used for the optical sensing of metal ions. *N. Carbon Mater.* **2016**, *31*, 135–143. [CrossRef]
107. Shuaib, E.; Shafi, P.M.; Yogesh, G.K.; Bose, A.C.; Sastikumar, D. Carbon nanoparticles synthesized by laser ablation of coconut shell charcoal in liquids for glucose sensing applications. *Mater. Res. Express* **2019**, *6*, 115610. [CrossRef]
108. Doñate-Buendía, C.; Fernández-Alonso, M.; Lancis, J.; Mínguez-Vega, G. Pulsed laser ablation in liquids for the production of gold nanoparticles and carbon quantum dots: From plasmonic to fluorescence and cell labelling. *J. Phys. Conf. Ser.* **2020**, *1537*, 012013. [CrossRef]
109. Hu, Z.; Jiao, X.-Y.; Xu, L. The N, S co-doped carbon dots with excellent luminescent properties from green tea leaf residue and its sensing of gefitinib. *Microchem. J.* **2020**, *154*, 104588. [CrossRef]
110. Yao, S.; Hu, Y.; Li, G. A one-step sonoelectrochemical preparation method of pure blue fluorescent carbon nanoparticles under a high intensity electric field. *Carbon* **2014**, *66*, 77–83. [CrossRef]
111. Liu, M.; Xu, Y.; Niu, F.; Gooding, J.J.; Liu, J. Carbon quantum dots directly generated from electrochemical oxidation of graphite electrodes in alkaline alcohols and the applications for specific ferric ion detection and cell imaging. *Analyst* **2016**, *141*, 2657–2664. [CrossRef] [PubMed]
112. Wu, Y.; Liu, Y.; Yin, J.; Li, H.; Huang, J. Facile ultrasonic synthesized NH_2-carbon quantum dots for ultrasensitive Co^{2+} ion detection and cell imaging. *Talanta* **2019**, *205*, 120121. [CrossRef] [PubMed]

113. He, C.; Yan, H.; Li, X.; Wang, X. In situ fabrication of carbon dots-based lubricants using a facile ultrasonic approach. *Green Chem.* **2019**, *21*, 2279–2285. [CrossRef]
114. Han, C.; Wang, R.; Wang, K.; Xu, H.; Sui, M.; Li, J.; Xu, K. Highly fluorescent carbon dots as selective and sensitive "on-off-on" probes for iron (III) ion and apoferritin detection and imaging in living cells. *Biosens. Bioelectron.* **2016**, *83*, 229–236. [CrossRef] [PubMed]
115. Edison, T.N.J.I.; Atchudan, R.; Sethuraman, M.G.; Shim, J.-J.; Lee, Y.R. Microwave assisted green synthesis of fluorescent N-doped carbon dots: Cytotoxicity and bio-imaging applications. *J. Photochem. Photobiol. B Biol.* **2016**, *161*, 154–161. [CrossRef]
116. Gu, D.; Shang, S.; Yu, Q.; Shen, J. Green synthesis of nitrogen-doped carbon dots from lotus root for Hg (II) ions detection and cell imaging. *Appl. Surf. Sci.* **2016**, *390*, 38–42. [CrossRef]
117. Hinterberger, V.; Wang, W.; Damm, C.; Wawra, S.; Thoma, M.; Peukert, W. Microwave-assisted one-step synthesis of white light-emitting carbon dot suspensions. *Opt. Mater.* **2018**, *80*, 110–119. [CrossRef]
118. Monte-Filho, S.S.; Andrade, S.I.; Lima, M.B.; Araujo, M.C. Synthesis of highly fluorescent carbon dots from lemon and onion juices for determination of riboflavin in multivitamin/mineral supplements. *J. Pharm. Anal.* **2019**, *9*, 209–216. [CrossRef] [PubMed]
119. Bano, D.; Kumar, V.; Singh, V.K.; Hasan, S.H. Green synthesis of fluorescent carbon quantum dots for the detection of mercury (II) and glutathione. *N. J. Chem.* **2018**, *42*, 5814–5821. [CrossRef]
120. Liu, Y.; Zhou, Q.; Yuan, Y.; Wu, Y. Hydrothermal synthesis of fluorescent carbon dots from sodium citrate and polyacrylamide and their highly selective detection of lead and pyrophosphate. *Carbon* **2017**, *115*, 550–560. [CrossRef]
121. Shen, J.; Shang, S.; Chen, X.; Wang, D.; Cai, Y. Facile synthesis of fluorescence carbon dots from sweet potato for Fe^{3+} sensing and cell imaging. *Mater. Sci. Eng. C* **2017**, *76*, 856–864. [CrossRef]
122. Xu, H.; Yang, X.; Li, G.; Zhao, C.; Liao, X. Green synthesis of fluorescent carbon dots for selective detection of tartrazine in food samples. *J. Agric. Food Chem.* **2015**, *63*, 6707–6714. [CrossRef]
123. Wang, H.; Lu, Q.; Hou, Y.; Liu, Y.; Zhang, Y. High fluorescence S, N co-doped carbon dots as an ultra-sensitive fluorescent probe for the determination of uric acid. *Talanta* **2016**, *155*, 62–69. [CrossRef]
124. Mehta, V.N.; Jha, S.; Basu, H.; Singhal, R.K.; Kailasa, S.K. One-step hydrothermal approach to fabricate carbon dots from apple juice for imaging of mycobacterium and fungal cells. *Sens. Actuators B Chem.* **2015**, *213*, 434–443. [CrossRef]
125. Paul, A.; Kurian, M. N-doped photoluminescent carbon dots from water hyacinth for tumour detection. *Mater. Today: Proc.* **2020**, *25*, 213–217. [CrossRef]
126. Xu, Q.; Li, W.; Ding, L.; Yang, W.; Xiao, H.; Ong, W.-J. Function-driven engineering of 1D carbon nanotubes and 0D carbon dots: Mechanism, properties and applications. *Nanoscale* **2019**, *11*, 1475–1504. [CrossRef]
127. Pirsaheb, M.; Moradi, S.; Shahlaei, M.; Farhadian, N. Application of carbon dots as efficient catalyst for the green oxidation of phenol: Kinetic study of the degradation and optimization using response surface methodology. *J. Hazard. Mater.* **2018**, *353*, 444–453. [CrossRef]
128. Lin, J.; Peng, Z.; Liu, Y.; Ruiz-Zepeda, F.; Ye, R.; Samuel, E.L.; Yacaman, M.J.; Yakobson, B.I.; Tour, J.M. Laser-induced porous graphene films from commercial polymers. *Nat. Commun.* **2014**, *5*, 5714. [CrossRef] [PubMed]
129. Sun, Z.; Yan, Z.; Yao, J.; Beitler, E.; Zhu, Y.; Tour, J.M. Growth of graphene from solid carbon sources. *Nature* **2010**, *468*, 549–552. [CrossRef]
130. Antunes, E.; De Resende, V.; Mengui, U.; Cunha, J.; Corat, E.; Massi, M. Analyses of residual iron in carbon nanotubes produced by camphor/ferrocene pyrolysis and purified by high temperature annealing. *Appl. Surf. Sci.* **2011**, *257*, 8038–8043. [CrossRef]
131. Kumar, M.; Ando, Y. A simple method of producing aligned carbon nanotubes from an unconventional precursor—Camphor. *Chem. Phys. Lett.* **2003**, *374*, 521–526. [CrossRef]
132. Sharon, M.; Hsu, W.; Kroto, H.; Walton, D.; Kawahara, A.; Ishihara, T.; Takita, Y. Camphor-based carbon nanotubes as an anode in lithium secondary batteries. *J. Power Sources* **2002**, *104*, 148–153. [CrossRef]
133. Antunes, E.; Almeida, E.; Rosa, C.; de Medeiros, L.; Pardini, L.; Massi, M.; Corat, E. Thermal annealing and electrochemical purification of multi-walled carbon nanotubes produced by camphor/ferrocene mixtures. *J. Nanosci. Nanotechnol.* **2010**, *10*, 1296–1303. [CrossRef]
134. Yang, X.; Wang, D.; Luo, N.; Feng, M.; Peng, X.; Liao, X. Green synthesis of fluorescent N, S-carbon dots from bamboo leaf and the interaction with nitrophenol compounds. *Spectrochim. Acta Part A Mol. Biomol. Spectrosc.* **2020**, *239*, 118462. [CrossRef]
135. Murugan, N.; Sundramoorthy, A.K. Green synthesis of fluorescent carbon dots from Borassus flabellifer flowers for label-free highly selective and sensitive detection of Fe^{3+} ions. *New J. Chem.* **2018**, *42*, 13297–13307. [CrossRef]
136. Huang, Q.; Li, Q.; Chen, Y.; Tong, L.; Lin, X.; Zhu, J.; Tong, Q. High quantum yield nitrogen-doped carbon dots: Green synthesis and application as "off-on" fluorescent sensors for the determination of Fe^{3+} and adenosine triphosphate in biological samples. *Sens. Actuators B Chem.* **2018**, *276*, 82–88. [CrossRef]
137. Sobhani, R.; Rezaei, B.; Shahshahanipour, M.; Ensafi, A.A.; Mohammadnezhad, G. Simple and green synthesis of carbon dots (CDs) from valerian root and application of modified mesoporous boehmite (AlOOH) with CDs as a fluorescence probe for determination of imipramine. *Anal. Bioanal. Chem.* **2019**, *411*, 3115–3124. [CrossRef] [PubMed]
138. Lotfy, W.A.; Ghanem, K.M.; El-Helow, E.R. Citric acid production by a novel Aspergillus niger isolate: II. Optimization of process parameters through statistical experimental designs. *Bioresour. Technol.* **2007**, *98*, 3470–3477. [CrossRef]
139. Kumar, R.; Yadav, R.M.; Awasthi, K.; Tiwari, R.; Srivastava, O. Effect of nitrogen variation on the synthesis of vertically aligned bamboo-shaped c–n nanotubes using sunflower oil. *Int. J. Nanosci.* **2011**, *10*, 809–813. [CrossRef]

140. Seo, D.H.; Rider, A.E.; Han, Z.J.; Kumar, S.; Ostrikov, K. Plasma break-down and Re-build: Same functional vertical graphenes from diverse natural precursors. *Adv. Mater.* **2013**, *25*, 5638–5642. [CrossRef] [PubMed]
141. Wang, J.; Wang, C.F.; Chen, S. Amphiphilic egg-derived carbon dots: Rapid plasma fabrication, pyrolysis process, and multicolor printing patterns. *Angew. Chem. Int. Ed.* **2012**, *51*, 9297–9301. [CrossRef]
142. Arabi, S.M.S.; Lalehloo, R.S.; Olyai, M.R.T.B.; Ali, G.A.; Sadegh, H. Removal of congo red azo dye from aqueous solution by ZnO nanoparticles loaded on multiwall carbon nanotubes. *Phys. E Low-Dimens. Syst. Nanostruct.* **2019**, *106*, 150–155. [CrossRef]
143. Sadegh, H.; Zare, K.; Maazinejad, B.; Shahryari-Ghoshekandi, R.; Tyagi, I.; Agarwal, S.; Gupta, V.K. Synthesis of MWCNT-COOH-Cysteamine composite and its application for dye removal. *J. Mol. Liq.* **2016**, *215*, 221–228. [CrossRef]
144. Naushad, M.; Ahamad, T.; Al-Maswari, B.M.; Alqadami, A.A.; Alshehri, S.M. Nickel ferrite bearing nitrogen-doped mesoporous carbon as efficient adsorbent for the removal of highly toxic metal ion from aqueous medium. *Chem. Eng. J.* **2017**, *330*, 1351–1360. [CrossRef]
145. Naushad, M. Surfactant assisted nano-composite cation exchanger: Development, characterization and applications for the removal of toxic Pb^{2+} from aqueous medium. *Chem. Eng. J.* **2014**, *235*, 100–108. [CrossRef]
146. Naushad, M.; Ahamad, T.; Sharma, G.; Ala'a, H.; Albadarin, A.B.; Alam, M.M.; ALOthman, Z.A.; Alshehri, S.M.; Ghfar, A.A. Synthesis and characterization of a new starch/SnO_2 nanocomposite for efficient adsorption of toxic Hg^{2+} metal ion. *Chem. Eng. J.* **2016**, *300*, 306–316. [CrossRef]
147. Sharma, G.; Kumar, A.; Naushad, M.; García-Peñas, A.; Ala'a, H.; Ghfar, A.A.; Sharma, V.; Ahamad, T.; Stadler, F.J. Fabrication and characterization of Gum arabic-cl-poly (acrylamide) nanohydrogel for effective adsorption of crystal violet dye. *Carbohydr. Polym.* **2018**, *202*, 444–453. [CrossRef]
148. Siddiqui, S.I.; Manzoor, O.; Mohsin, M.; Chaudhry, S.A. Nigella sativa seed based nanocomposite-MnO_2/BC: An antibacterial material for photocatalytic degradation, and adsorptive removal of Methylene blue from water. *Environ. Res.* **2019**, *171*, 328–340. [CrossRef]
149. Thakur, M.; Sharma, G.; Ahamad, T.; Ghfar, A.A.; Pathania, D.; Naushad, M. Efficient photocatalytic degradation of toxic dyes from aqueous environment using gelatin-Zr (IV) phosphate nanocomposite and its antimicrobial activity. *Colloids Surf. B Biointerfaces* **2017**, *157*, 456–463. [CrossRef] [PubMed]
150. Ahamad, T.; Naushad, M.; Eldesoky, G.E.; Al-Saeedi, S.I.; Nafady, A.; Al-Kadhi, N.S.; Ala'a, H.; Khan, A.A.; Khan, A. Effective and fast adsorptive removal of toxic cationic dye (MB) from aqueous medium using amino-functionalized magnetic multiwall carbon nanotubes. *J. Mol. Liq.* **2019**, *282*, 154–161. [CrossRef]
151. Zhang, X.; Cao, S.; Wu, Z.; Zhao, S.; Piao, L. Enhanced photocatalytic activity towards degradation and H_2 evolution over one dimensional TiO_2@MWCNTs heterojunction. *Appl. Surf. Sci.* **2017**, *402*, 360–368. [CrossRef]
152. Saharan, P.; Sharma, A.K.; Kumar, V.; Kaushal, I. Multifunctional CNT supported metal doped MnO_2 composite for adsorptive removal of anionic dye and thiourea sensing. *Mater. Chem. Phys.* **2019**, *221*, 239–249. [CrossRef]
153. Wu, J.; Liu, B.; Ren, Z.; Ni, M.; Li, C.; Gong, Y.; Qin, W.; Huang, Y.; Sun, C.Q.; Liu, X. CuS/RGO hybrid photocatalyst for full solar spectrum photoreduction from UV/Vis to near-infrared light. *J. Colloid Interface Sci.* **2018**, *517*, 80–85. [CrossRef] [PubMed]
154. Nguyen, C.H.; Juang, R.-S. Efficient removal of methylene blue dye by a hybrid adsorption–photocatalysis process using reduced graphene oxide/titanate nanotube composites for water reuse. *J. Ind. Eng. Chem.* **2019**, *76*, 296–309. [CrossRef]
155. Zhang, H.; Ming, H.; Lian, S.; Huang, H.; Li, H.; Zhang, L.; Liu, Y.; Kang, Z.; Lee, S.-T. Fe_2O_3/carbon quantum dots complex photocatalysts and their enhanced photocatalytic activity under visible light. *Dalton Trans.* **2011**, *40*, 10822–10825. [CrossRef] [PubMed]
156. Sathe, B.R.; Zou, X.; Asefa, T. Metal-free B-doped graphene with efficient electrocatalytic activity for hydrogen evolution reaction. *Catal. Sci. Technol.* **2014**, *4*, 2023–2030. [CrossRef]
157. Zhou, W.; Zhou, Y.; Yang, L.; Huang, J.; Ke, Y.; Zhou, K.; Li, L.; Chen, S. N-doped carbon-coated cobalt nanorod arrays supported on a titanium mesh as highly active electrocatalysts for the hydrogen evolution reaction. *J. Mater. Chem. A* **2015**, *3*, 1915–1919. [CrossRef]
158. Duan, J.; Chen, S.; Jaroniec, M.; Qiao, S.Z. Porous C_3N_4 nanolayers@N-graphene films as catalyst electrodes for highly efficient hydrogen evolution. *ACS Nano* **2015**, *9*, 931–940. [CrossRef]
159. Liu, Q.; Chen, T.; Guo, Y.; Zhang, Z.; Fang, X. Ultrathin g-C_3N_4 nanosheets coupled with carbon nanodots as 2D/0D composites for efficient photocatalytic H_2 evolution. *Appl. Catal. B Environ.* **2016**, *193*, 248–258. [CrossRef]
160. Zhang, X.; Sun, Y.; Cui, X.; Jiang, Z. A green and facile synthesis of TiO_2/graphene nanocomposites and their photocatalytic activity for hydrogen evolution. *Int. J. Hydrogen Energy* **2012**, *37*, 811–815. [CrossRef]
161. Freddi, S.; Emelianov, A.V.; Bobrinetskiy, I.I.; Drera, G.; Pagliara, S.; Kopylova, D.S.; Chiesa, M.; Santini, G.; Mores, N.; Moscato, U. Development of a sensing array for human breath analysis based on SWCNT layers functionalized with semiconductor organic molecules. *Adv. Healthc. Mater.* **2020**, *9*, 2000377. [CrossRef] [PubMed]
162. Lin, T.; Lv, X.; Hu, Z.; Xu, A.; Feng, C. Semiconductor metal oxides as chemoresistive sensors for detecting volatile organic compounds. *Sensors* **2019**, *19*, 233. [CrossRef] [PubMed]
163. Kumar, P.; Kim, K.-H.; Mehta, P.K.; Ge, L.; Lisak, G. Progress and challenges in electrochemical sensing of volatile organic compounds using metal-organic frameworks. *Crit. Rev. Environ. Sci. Technol.* **2019**, *49*, 2016–2048. [CrossRef]
164. Tripathi, K.M.; Kim, T.; Losic, D.; Tung, T.T. Recent advances in engineered graphene and composites for detection of volatile organic compounds (VOCs) and non-invasive diseases diagnosis. *Carbon* **2016**, *110*, 97–129. [CrossRef]

165. Chen, W.Y.; Lai, S.-N.; Yen, C.-C.; Jiang, X.; Peroulis, D.; Stanciu, L.A. Surface functionalization of Ti_3C_2T x MXene with highly reliable superhydrophobic protection for volatile organic compounds sensing. *ACS Nano* **2020**, *14*, 11490–11501. [CrossRef]
166. Wang, D.; Tian, L.; Li, H.; Wan, K.; Yu, X.; Wang, P.; Chen, A.; Wang, X.; Yang, J. Mesoporous ultrathin SnO_2 nanosheets in situ modified by graphene oxide for extraordinary formaldehyde detection at low temperatures. *ACS Appl. Mater. Interfaces* **2019**, *11*, 12808–12818. [CrossRef]
167. Rong, X.; Chen, D.; Qu, G.; Li, T.; Zhang, R.; Sun, J. Effects of graphene on the microstructures of SnO_2@rGO nanocomposites and their formaldehyde-sensing performance. *Sens. Actuators B Chem.* **2018**, *269*, 223–237. [CrossRef]
168. Anasori, B.; Lukatskaya, M.R.; Gogotsi, Y. 2D metal carbides and nitrides (MXenes) for energy storage. *Nat. Rev. Mater.* **2017**, *2*, 16098. [CrossRef]
169. Naguib, M.; Kurtoglu, M.; Presser, V.; Lu, J.; Niu, J.; Heon, M.; Hultman, L.; Gogotsi, Y.; Barsoum, M.W. Two-dimensional nanocrystals produced by exfoliation of Ti_3AlC_2. *Adv. Mater.* **2011**, *23*, 4248–4253. [CrossRef]
170. Naguib, M.; Mochalin, V.N.; Barsoum, M.W.; Gogotsi, Y. 25th anniversary article: MXenes: A new family of two-dimensional materials. *Adv. Mater.* **2014**, *26*, 992–1005. [CrossRef]
171. Naguib, M.; Mashtalir, O.; Carle, J.; Presser, V.; Lu, J.; Hultman, L.; Gogotsi, Y.; Barsoum, M.W. Two-dimensional transition metal carbides. *ACS Nano* **2012**, *6*, 1322–1331. [CrossRef] [PubMed]
172. Koh, H.-J.; Kim, S.J.; Maleski, K.; Cho, S.-Y.; Kim, Y.-J.; Ahn, C.W.; Gogotsi, Y.; Jung, H.-T. Enhanced selectivity of MXene gas sensors through metal ion intercalation: In situ X-ray diffraction study. *ACS Sens.* **2019**, *4*, 1365–1372. [CrossRef] [PubMed]
173. Chen, W.Y.; Jiang, X.; Lai, S.-N.; Peroulis, D.; Stanciu, L. Nanohybrids of a MXene and transition metal dichalcogenide for selective detection of volatile organic compounds. *Nat. Commun.* **2020**, *11*, 1302. [CrossRef] [PubMed]
174. Zou, S.; Gao, J.; Liu, L.; Lin, Z.; Fu, P.; Wang, S.; Chen, Z. Enhanced gas sensing properties at low working temperature of iron molybdate/MXene composite. *J. Alloys Compd.* **2020**, *817*, 152785. [CrossRef]
175. Ashfaq, M.; Verma, N.; Khan, S. Copper/zinc bimetal nanoparticles-dispersed carbon nanofibers: A novel potential antibiotic material. *Mater. Sci. Eng. C* **2016**, *59*, 938–947. [CrossRef] [PubMed]
176. Anjum, M.; Miandad, R.; Waqas, M.; Gehany, F.; Barakat, M. Remediation of wastewater using various nano-materials. *Arab. J. Chem.* **2019**, *12*, 4897–4919. [CrossRef]
177. Ashfaq, M.; Verma, N.; Khan, S. Highly effective Cu/Zn-carbon micro/nanofiber-polymer nanocomposite-based wound dressing biomaterial against the *P. aeruginosa* multi-and extensively drug-resistant strains. *Mater. Sci. Eng. C* **2017**, *77*, 630–641. [CrossRef]
178. Awasthi, S.; Ashfaq, M.; Singh, S. Effect of glucose and chloramphenicol on ABS biodegradation by a bacterial consortium. *Biol. Med.* **2009**, *1*, 15–19.
179. Ayangbenro, A.S.; Babalola, O.O. A new strategy for heavy metal polluted environments: A review of microbial biosorbents. *Int. J. Environ. Res. Public Health* **2017**, *14*, 94. [CrossRef] [PubMed]
180. Bhattacharya, K.; Mukherjee, S.P.; Gallud, A.; Burkert, S.C.; Bistarelli, S.; Bellucci, S.; Bottini, M.; Star, A.; Fadeel, B. Biological interactions of carbon-based nanomaterials: From coronation to degradation. *Nanomed. Nanotechnol. Biol. Med.* **2016**, *12*, 333–351. [CrossRef]
181. Bhuyan, M.; Uddin, M.; Islam, M.; Bipasha, F.; Hossain, S. Synthesis of graphene. *Int. Nano Lett.* **2016**, *6*, 65–83. [CrossRef]
182. Chauhan, D.; Jaiswal, M.; Sankararamakrishnan, N. Removal of cadmium and hexavalent chromium from electroplating waste water using thiocarbamoyl chitosan. *Carbohydr. Polym.* **2012**, *88*, 670–675. [CrossRef]
183. Chauhan, D.; Afreen, S.; Mishra, S.; Sankararamakrishnan, N. Synthesis, characterization and application of zinc augmented aminated PAN nanofibers towards decontamination of chemical and biological contaminants. *J. Ind. Eng. Chem.* **2017**, *55*, 50–64. [CrossRef]
184. Chen, Q.; Dai, L.; Gao, M.; Huang, S.; Mau, A. Plasma activation of carbon nanotubes for chemical modification. *J. Phys. Chem. B* **2001**, *105*, 618–622. [CrossRef]
185. Khan, I.; Saeed, K.; Khan, I. Nanoparticles: Properties, applications and toxicities. *Arab. J. Chem.* **2019**, *12*, 908–931. [CrossRef]
186. Khare, P.; Talreja, N.; Deva, D.; Sharma, A.; Verma, N. Carbon nanofibers containing metal-doped porous carbon beads for environmental remediation applications. *Chem. Eng. J.* **2013**, *229*, 72–81. [CrossRef]
187. Liu, M.; Yang, Y.; Zhu, T.; Liu, Z. A general approach to chemical modification of single-walled carbon nanotubes with peroxy organic acids and its application in polymer grafting. *J. Phys. Chem. C* **2007**, *111*, 2379–2385. [CrossRef]
188. Liu, C.; Yu, Z.; Neff, D.; Zhamu, A.; Jang, B.Z. Graphene-based supercapacitor with an ultrahigh energy density. *Nano Lett.* **2010**, *10*, 4863–4868. [CrossRef]
189. Lu, G.; Yu, K.; Wen, Z.; Chen, J. Semiconducting graphene: Converting graphene from semimetal to semiconductor. *Nanoscale* **2013**, *5*, 1353–1368. [CrossRef]
190. Lu, P.; Xue, D.; Yang, H.; Liu, Y. Supercapacitor and nanoscale research towards electrochemical energy storage. *Int. J. Smart Nano Mater.* **2013**, *4*, 2–26. [CrossRef]
191. Lukatskaya, M.R.; Dunn, B.; Gogotsi, Y. Multidimensional materials and device architectures for future hybrid energy storage. *Nat. Commun.* **2016**, *7*, 12647. [CrossRef]
192. Visakh, P. Introduction for Nanomaterials and Nanocomposites: State of Art, New Challenges, and Opportunities. In *Nanomaterials and Nanocomposites: Zero-to Three-Dimensional Materials and Their Composites*; Wiley: Hoboken, NJ, USA, 2016; pp. 1–20.
193. Wang, J.; Kaskel, S. KOH activation of carbon-based materials for energy storage. *J. Mater. Chem.* **2012**, *22*, 23710–23725. [CrossRef]

194. Wang, X.; Ouyang, Y.; Li, X.; Wang, H.; Guo, J.; Dai, H. Room-temperature all-semiconducting sub-10-nm graphene nanoribbon field-effect transistors. *Phys. Rev. Lett.* **2008**, *100*, 206803. [CrossRef] [PubMed]
195. Wu, Z.; Li, L.; Yan, J.M.; Zhang, X.B. Materials design and system construction for conventional and new-concept supercapacitors. *Adv. Sci.* **2017**, *4*, 1600382. [CrossRef]
196. Zheng, X.; Zhang, L. Photonic nanostructures for solar energy conversion. *Energy Environ. Sci.* **2016**, *9*, 2511–2532. [CrossRef]
197. Zheng, J.; Shao, M.; Che, W.; Zhang, L.; Zhong, L.; Zhang, Y.; Streets, D. Speciated VOC emission inventory and spatial patterns of ozone formation potential in the Pearl River Delta, China. *Environ. Sci. Technol.* **2009**, *43*, 8580–8586. [CrossRef] [PubMed]
198. Zheng, J.-S.; Zhang, L.; Shellikeri, A.; Cao, W.; Wu, Q.; Zheng, J.P. A hybrid electrochemical device based on a synergetic inner combination of Li ion battery and Li ion capacitor for energy storage. *Sci. Rep.* **2017**, *7*, 1–8. [CrossRef]
199. TermehYousefi, A.; Bagheri, S.; Shinji, K.; Rouhi, J.; Rusop Mahmood, M.; Ikeda, S. Fast synthesis of multilayer carbon nanotubes from camphor oil as an energy storage material. *Bio. Med. Res. Int.* **2014**, *2014*, 691537. [CrossRef]
200. Tostado-Plascencia, M.M.; Sanchez-Tizapa, M.; Zamudio-Ojeda, A. Synthesis and characterization of multiwalled carbon nanotubes functionalized with chlorophyll-derivatives compounds extracted from Hibiscus tiliaceus. *Diam. Relat. Mater.* **2018**, *89*, 151–162. [CrossRef]
201. Maddinedi, S.B.; Mandal, B.K.; Vankayala, R.; Kalluru, P.; Pamanji, S.R. Bioinspired reduced graphene oxide nanosheets using Terminalia chebula seeds extract. *Spectrochim. Acta Part A Mol. Biomol. Spectrosc.* **2015**, *145*, 117–124. [CrossRef]
202. Jin, X.; Li, N.; Weng, X.; Li, C.; Chen, Z. Green reduction of graphene oxide using eucalyptus leaf extract and its application to remove dye. *Chemosphere* **2018**, *208*, 417–424. [CrossRef] [PubMed]
203. Thongsai, N.; Tanawannapong, N.; Praneerad, J.; Kladsomboon, S.; Jaiyong, P.; Paoprasert, P. Real-time detection of alcohol vapors and volatile organic compounds via optical electronic nose using carbon dots prepared from rice husk and density functional theory calculation. *Colloids Surf. A Physicochem. Eng. Asp.* **2019**, *560*, 278–287. [CrossRef]
204. Singh, V.; Chatterjee, S.; Palecha, M.; Sen, P.; Ateeq, B.; Verma, V. Chickpea peel waste as sustainable precursor for synthesis of fluorescent carbon nanotubes for bioimaging application. *Carbon Lett.* **2021**, *31*, 117–123. [CrossRef]
205. Wongso, V.; Sambudi, N.S.; Sufian, S. The effect of hydrothermal conditions on photoluminescence properties of rice husk-derived silica-carbon quantum dots for methylene blue degradation. *Biomass Convers. Biorefinery* **2021**, *11*, 2641–2654. [CrossRef]
206. Mehta, A.; Pooja, D.; Thakur, A.; Basu, S. Enhanced photocatalytic water splitting by gold carbon dot core shell nanocatalyst under visible/sunlight. *N. J. Chem.* **2017**, *41*, 4573–4581. [CrossRef]
207. Li, K.; Su, F.-Y.; Zhang, W.-D. Modification of g-C_3N_4 nanosheets by carbon quantum dots for highly efficient photocatalytic generation of hydrogen. *Appl. Surf. Sci.* **2016**, *375*, 110–117. [CrossRef]
208. Liu, S.; Liu, Z.; Li, Q.; Xia, H.; Yang, W.; Wang, R.; Li, Y.; Zhao, H.; Tian, B. Facile synthesis of carbon dots from wheat straw for colorimetric and fluorescent detection of fluoride and cellular imaging. *Spectrochim. Acta Part A Mol. Biomol. Spectrosc.* **2021**, *246*, 118964. [CrossRef] [PubMed]
209. Vandarkuzhali, S.A.A.; Natarajan, S.; Jeyabalan, S.; Sivaraman, G.; Singaravadivel, S.; Muthusubramanian, S.; Viswanathan, B. Pineapple peel-derived carbon dots: Applications as sensor, molecular keypad lock, and memory device. *ACS Omega* **2018**, *3*, 12584–12592. [CrossRef]
210. Praneerad, J.; Neungnoraj, K.; In, I.; Paoprasert, P. Environmentally friendly supercapacitor based on carbon dots from durian peel as an electrode. *Key Eng. Mater.* **2019**, *803*, 115–119. [CrossRef]
211. Aggarwal, R.; Saini, D.; Singh, B.; Kaushik, J.; Garg, A.K.; Sonkar, S.K. Bitter apple peel derived photoactive carbon dots for the sunlight induced photocatalytic degradation of crystal violet dye. *Sol. Energy* **2020**, *197*, 326–331. [CrossRef]
212. Zhou, M.; Wang, S.; Yang, P.; Huang, C.; Wang, X. Boron carbon nitride semiconductors decorated with CdS nanoparticles for photocatalytic reduction of CO_2. *ACS Catal.* **2018**, *8*, 4928–4936. [CrossRef]
213. Xie, S.; Su, H.; Wei, W.; Li, M.; Tong, Y.; Mao, Z. Remarkable photoelectrochemical performance of carbon dots sensitized TiO_2 under visible light irradiation. *J. Mater. Chem. A* **2014**, *2*, 16365–16368. [CrossRef]
214. Zhang, W.; Yang, S.; Jiang, M.; Hu, Y.; Hu, C.; Zhang, X.; Jin, Z. Nanocapillarity and nanoconfinement effects of pipet-like bismuth@ carbon nanotubes for highly efficient electrocatalytic CO_2 reduction. *Nano Lett.* **2021**, *21*, 2650–2657. [CrossRef]
215. Shetti, N.P.; Nayak, D.S.; Malode, S.J.; Kakarla, R.R.; Shukla, S.S.; Aminabhavi, T.M. Sensors based on ruthenium-doped TiO_2 nanoparticles loaded into multi-walled carbon nanotubes for the detection of flufenamic acid and mefenamic acid. *Anal. Chim. Acta* **2019**, *1051*, 58–72. [CrossRef] [PubMed]
216. Han, T.; Nag, A.; Mukhopadhyay, S.C.; Xu, Y. Carbon nanotubes and its gas-sensing applications: A review. *Sens. Actuators A Phys.* **2019**, *291*, 107–143. [CrossRef]
217. Zhang, K.; Zhao, Y.; Fu, D.; Chen, Y. Molybdenum carbide nanocrystal embedded N-doped carbon nanotubes as electrocatalysts for hydrogen generation. *J. Mater. Chem. A* **2015**, *3*, 5783–5788. [CrossRef]
218. Fan, L.; Tang, L.; Gong, H.; Yao, Z.; Guo, R. Carbon-nanoparticles encapsulated in hollow nickel oxides for supercapacitor application. *J. Mater. Chem.* **2012**, *22*, 16376–16381. [CrossRef]
219. Nagamuthu, S.; Vijayakumar, S.; Muralidharan, G. Synthesis of Mn_3O_4/amorphous carbon nanoparticles as electrode material for high performance supercapacitor applications. *Energy Fuels* **2013**, *27*, 3508–3515. [CrossRef]
220. Sadhanala, H.K.; Nanda, K.K. Boron-doped carbon nanoparticles: Size-independent color tunability from red to blue and bioimaging applications. *Carbon* **2016**, *96*, 166–173. [CrossRef]